

# **Optimization of Acoustic Source Locations for Enhanced Performance in Radio Acoustic Sounding Systems**

Dissertation submitted in partial fulfillment of the requirements  
for the award of the degree of

**Bachelor of Technology**

by

**Yapati Murali Sai**

(Roll No. 2021AMB009)

Under the Supervision of

**Dr. T. V. Chandrasekhar Sarma**

Scientist/Engineer - G, ASBID

**NATIONAL ATMOSPHERIC RESEARCH LABORATORY**

**Department of Space, Govt. of India, Gadanki, Tirupati**



Department of Aerospace Engineering and Applied Mechanics  
**INDIAN INSTITUTE OF ENGINEERING SCIENCE AND  
TECHNOLOGY SHIBPUR**

**Howrah - 711 103. West Bengal, India**

**May 20 - July 16, 2024**



# **Dissertation Approval**

This thesis entitled **Optimizing Acoustic Sources for Enhanced Performance in Radio Acoustic Sounding Systems** by **Yapati Murali Sai**, Roll No. **2021AMB009** is approved for the degree of **Degree (B.Tech)** from the Indian Institute of Engineering Science and Technology, Shibpur.

.....  
Dr. T. V. Chandrasekhar Sarma  
(Supervisor)

Date: 16 July, 2024  
Place: NARL Tirupati

# **Declaration**

I declare that this written submission represents my ideas in my own words. Where others' ideas and words have been included, I have adequately cited and referenced the source. I declare that I have adhered to all academic honesty and integrity principles and have not misrepresented, fabricated, or falsified any idea/data/fact/source in my submission. I understand that any violation of the above will cause disciplinary action by the Institute and can also evoke penal action from the source that has thus not been properly cited or from whom proper permission has not been taken when needed.

**Signature of Student:** Ypati Murali Sai

Ypati Murali Sai

Roll No.: 2021AMB009

Date: 16-07-2024

Place: IEST Shibpur

# Abstract

This project presents an optimized approach for enhancing the height coverage of virtual temperature profiles using the Radio Acoustic Sounding System (RASS). The primary challenge in maximizing height coverage with the influence of wind, which distorts the acoustic wavefronts and shifts them away from the sensing volume, reducing the effectiveness of backscatter to the radar antenna. To address this, we employ ray-tracing techniques to model the propagation of acoustic wavefronts in an inhomogeneous atmosphere, considering the effects of temperature gradients and horizontal wind.

Our method involves designing an acoustic source that maintains continuous height coverage within the radar antenna array, ensuring optimal alignment of the radar and acoustic wave vectors. By analyzing the propagation paths of acoustic waves and their interaction with atmospheric conditions, we identify the portions of wavefronts that contribute to effective backscatter within the 130m x 130m MST radar antenna array. This allows for precise measurement of sound speed at various altitudes, from which ambient temperature profiles are derived.

Furthermore, we employ a frequency-chirped acoustic waveform to accommodate the changing speed of sound with altitude, ensuring consistent wavelength coverage and satisfying the Bragg scattering condition. This innovation improves the accuracy of temperature and wind profiling in the troposphere, contributing valuable data for studying atmospheric phenomena.

This report details the design, construction, and operation of the optimized acoustic source, along with the mechanical aspects of the instrument. Our results demonstrate significant improvements in height coverage and measurement accuracy, providing a robust tool for atmospheric research and enhancing our understanding of storm electrification and global energy exchange processes.

*Keywords:* RASS, Radar antenna alignment, Ray-tracing techniques, Atmospheric wavefronts, Virtual temperature profiles, Bragg scattering condition.



# Contents

<b>Abstract</b>	<b>i</b>
<b>1 Introduction</b>	<b>1</b>
1.1 Background . . . . .	1
1.2 Problem Statement . . . . .	6
1.3 Research objectives . . . . .	6
1.4 Need of the Study . . . . .	7
<b>2 Design Methodology</b>	<b>9</b>
2.1 Introduction . . . . .	9
2.1.1 Initial Data Collection . . . . .	9
2.1.2 Acoustic Source Placement Strategy . . . . .	9
2.1.3 Waveform Fitting and Surface Normal Calculation . . . . .	10
2.1.4 Effectiveness of this approach: . . . . .	35
2.2 Design Principles . . . . .	35
2.3 Flowchart . . . . .	37
2.4 Design Implementation . . . . .	38
<b>3 Results and Analysis</b>	<b>47</b>
3.1 Simulation . . . . .	47
3.2 Simulation Results . . . . .	47
3.3 Conclusion . . . . .	50
<b>Appendix A Codes and Developed Tools</b>	<b>51</b>
A.1 RASS Acoustic Source Location Optimization . . . . .	51
A.2 Simulation and Results Analysis . . . . .	52
<b>List of Tables</b>	<b>53</b>
<b>List of Figures</b>	<b>55</b>
<b>Acknowledgments</b>	<b>61</b>

# Chapter 1

## Introduction

### 1.1 Background

The study investigates the influences of atmospheric wind and temperature profiles on the maximum height attainable in temperature measurements using a Radio Acoustic Sounding System (RASS). RASS utilizes radar to receive echoes backscattered from periodic perturbations in the atmospheric refractive index produced by an incident acoustic pulse. This allows for the measurement of atmospheric temperature from the local speed of sound, which is derived from the Doppler frequency shift of the RASS echo signal. A crucial condition for efficient RASS echo backscatter in monostatic radar systems is that the radar beam must be incident normal to the perturbation wave surfaces, i.e., to the acoustic wavefront.

Radio Acoustic Sounding Systems (RASS) are employed to measure virtual temperature remotely, typically from the ground and usually in a vertical direction. While RASS has been in development since the 1970s, it only became widely used in the 1990s. An introduction to RASS techniques and their history can be found in the relevant literature. In summary, RASS employs radar to measure the speed of propagation of an acoustic disturbance and, from this, derive the virtual temperature. Virtual temperature refers to the temperature of dry air at the same density as moist ambient air and is the appropriate measure for air density. It can be slightly higher than kinetic temperature in very humid conditions.

RASS devices are now commercially available and are often deployed as attachments to

lower troposphere wind profilers for routine monitoring and research applications. Traditionally, atmospheric temperature has been measured using radiosondes, which are in-situ sensors carried by small balloons. However, remote sensing instruments like RASS offer significant advantages over radiosondes. RASS can perform continuous measurements at high time resolutions (minutes), while launching radiosondes even hourly is expensive and labor-intensive. Additionally, RASS measurements are inherently averaged over a large spatial domain providing a more reliable temperature estimate than the essentially one-dimensional radiosonde measurements.

This study aims to optimize the height coverage of virtual temperature profiles obtained using RASS by considering the effects of atmospheric wind and temperature variations. By enhancing the understanding of these influences, the study seeks to improve the efficiency and accuracy of RASS temperature measurements.

The hemispherical acoustic wavefronts generated by the exciter propagate vertically. They then meet an altitude gradient in temperature and a horizontal wind. As the temperature decreases with altitude, the propagation speed reduces, and the spherical wavefronts become ellipsoidal. Further, horizontal wind at each altitude affects the wavefront. the Bragg scattering requirement demands that the radar and acoustic wave vectors be aligned for effective backscatter to reach the antenna. However, the distorting effects of temperature gradient and wind would cause backscatter from considerable portions of the audio wavefronts to fall outside the antenna array. Acoustic propagation is represented as outward propagating rays to forecast the location of acoustic wavefronts that would result in backscatter falling within the antenna array. Ma-suda (1988) described the method of two-dimensional ray tracing. Warshaw (1980) provided a three-dimensional characterization of acoustic ray propagation in a heterogeneous atmosphere.

$$\frac{d}{dt}(x) = v_x + c_s \sin \theta \cos \varphi \quad (1.1)$$

$$\frac{d}{dt}(y) = v_y + c_s \sin \theta \sin \varphi \quad (1.2)$$

$$\frac{d}{dt}(z) = c_s \cos \theta \quad (1.3)$$

$$\frac{d\theta}{dt} = \sin \theta \left( \frac{\partial c_s}{\partial z} + \sin \theta \left( \cos \varphi \frac{\partial v_x}{\partial z} + \sin \varphi \frac{\partial v_y}{\partial z} \right) \right) \quad (1.4)$$

The equations predict that the azimuthal orientation of the wavefront normal along any given ray path does not change during the propagation as no time derivatives of phi are involved. Using these equations, the wavefronts without wind and temperature gradient would be hemispherical. Here is the measured temperature and wind from the radiosonde flight of 03 Dec 2007.

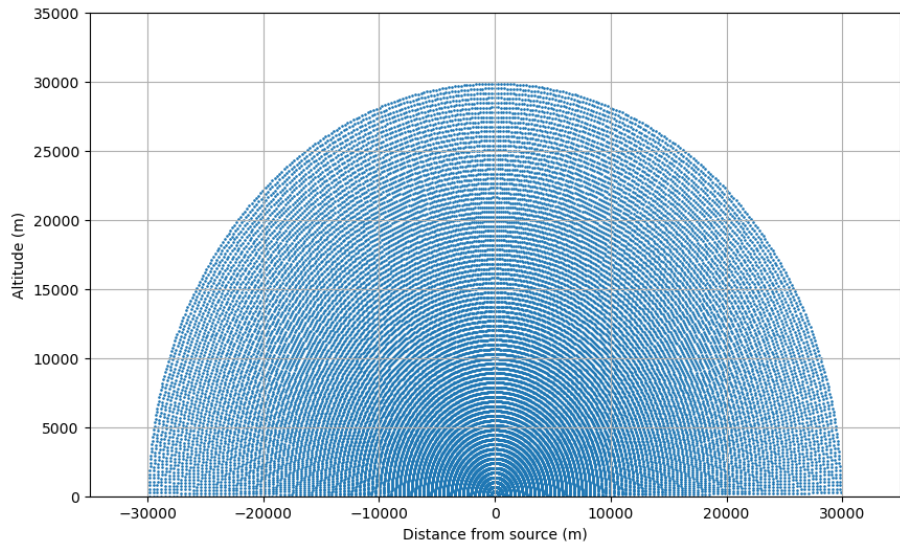


Figure 1.1: Acoustic wavefronts in the absence of wind and temperature

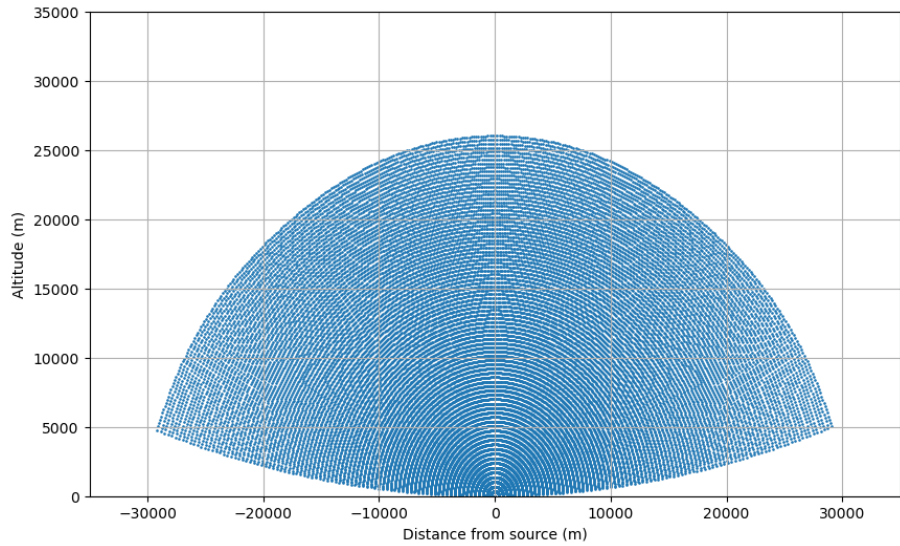


Figure 1.2: Acoustic wavefronts computer using temperature data

The effect on the wavefront keeping the wind zero. This is shown in figure 1.2. Further, the result of combined effects of wind and temperature in the EW and NS plane is shown in figure 1.3 and 1.4. Now from this figure, we keep those portions of the waveform that result in backscatter falling within the MST radar antenna array of size 130m x 130m, by tracing normals back to the radar antenna on the ground. This result for the EW and NS planes is shown respectively in figures 1.5 and 1.6.

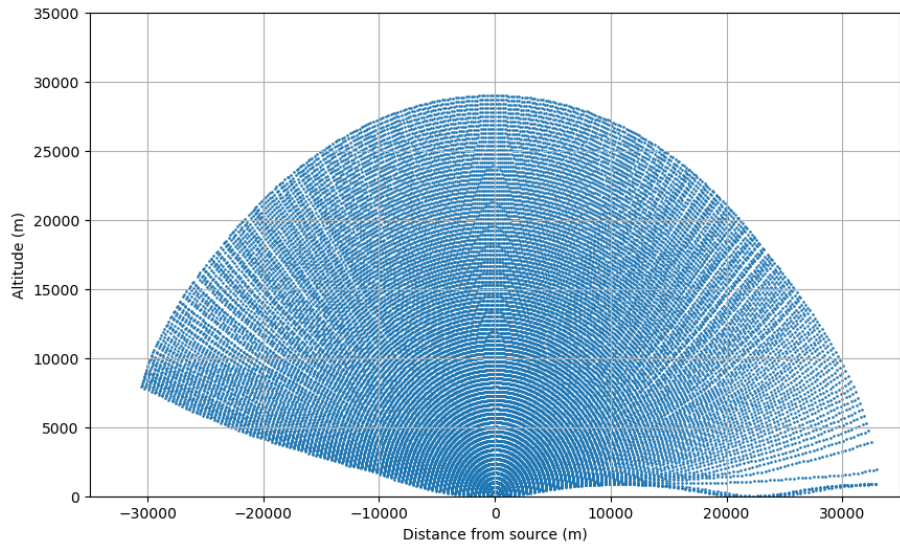


Figure 1.3: Acoustic wavefronts computer using temperature data and wind data in N-S direction

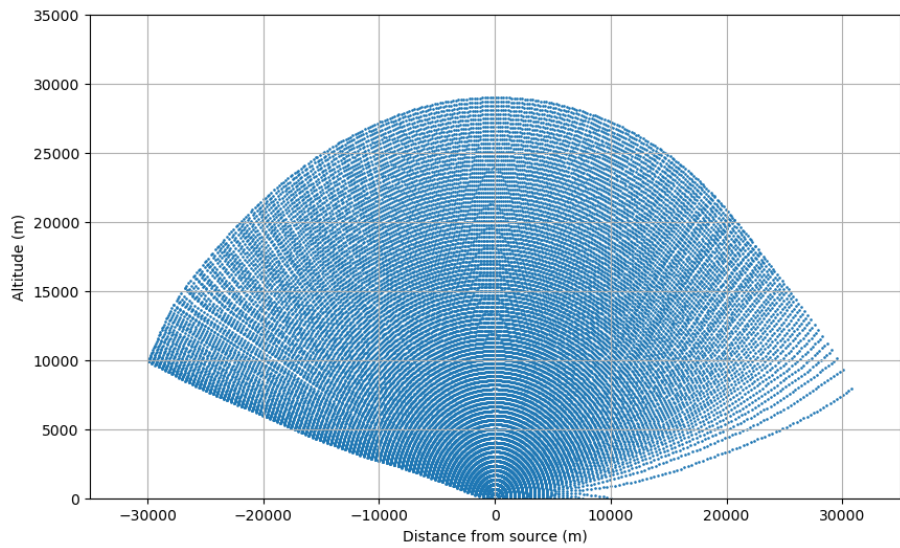


Figure 1.4: Acoustic wavefronts computer using temperature data and wind data in E-W direction

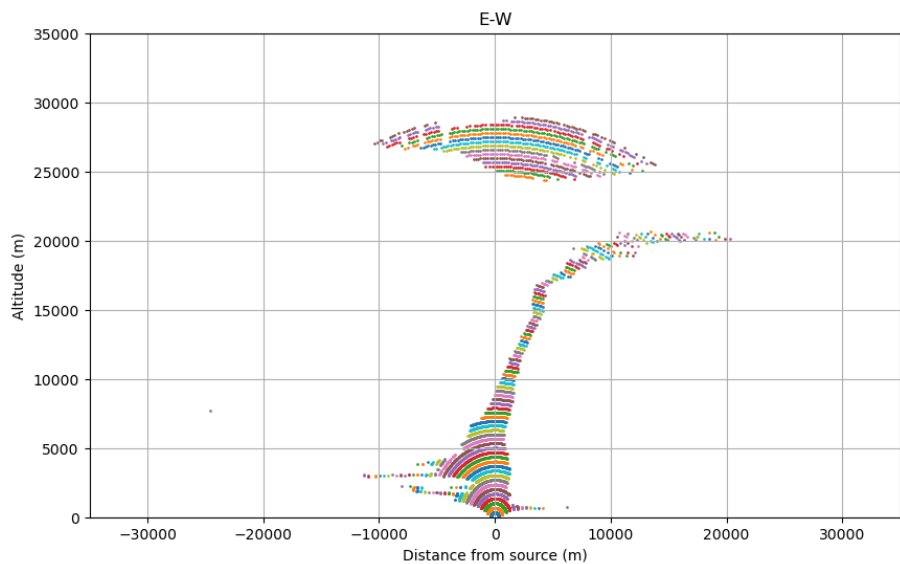


Figure 1.5: Portions of acoustic wavefronts in the EW plane from which backscatter would fall on the antenna array computed using the radiosonde flight data

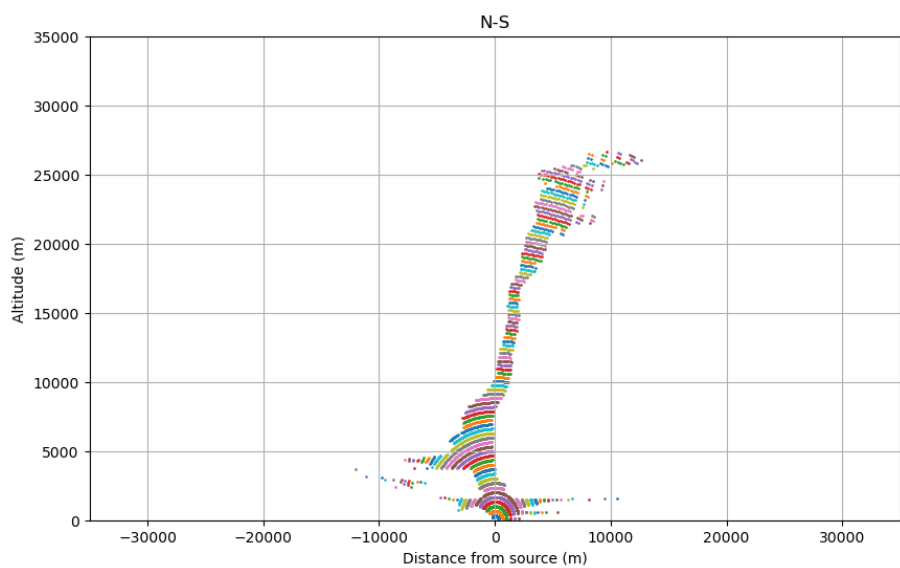


Figure 1.6: Portions of acoustic wavefronts in the NS plane from which backscatter would fall on the antenna array computed using the radiosonde flight data

## 1.2 Problem Statement

The effective height coverage of virtual temperature profiles obtained using the Radio Acoustic Sounding System (RASS) is critically limited by the distortion of acoustic wave fronts due to atmospheric conditions, specifically temperature gradients and horizontal winds. These distortions prevent a significant portion of the backscatter from aligning with the radar antenna array, thus reducing the accuracy and reliability of temperature and wind measurements at various altitudes. This project seeks to optimize the design and operation of the acoustic source locations to ensure continuous height coverage within the radar antenna's sensing volume, enhancing the effectiveness of RASS in profiling atmospheric conditions.

## 1.3 Research objectives

This study aims to optimize the design and operation of acoustic sources in Radio Acoustic Sounding Systems (RASS) to achieve continuous and accurate height coverage for atmospheric temperature and wind profiling. Specifically, the objectives include:

1. **Enhancing Height Coverage:** Develop methods to mitigate the impact of temperature gradients and horizontal winds on acoustic wave fronts, ensuring effective backscatter within radar antenna arrays.
2. **Improving Measurement Precision:** Implement innovative acoustic source designs that maintain alignment between radar and acoustic wave vectors, enhancing the reliability and accuracy of temperature and wind profiles.
3. **Reducing Operational Costs:** Optimize acoustic source technologies to streamline data collection processes, reducing operational expenses associated with atmospheric research and monitoring.
4. **Advancing Scientific Understanding:** Contribute new insights into atmospheric dynamics and their interactions with environmental factors, supporting advancements in meteorological science and weather prediction models.

These objectives outline the specific aims of the study in optimizing acoustic sources within RASS, addressing current limitations, and advancing capabilities in atmospheric profiling.

## 1.4 Need of the Study

The accurate measurement of atmospheric temperature and wind profiles is essential for understanding various meteorological phenomena, including storm electrification, climate dynamics, and global energy exchanges. Traditional methods of obtaining these measurements face several challenges, particularly in terms of height coverage and precision.

1. **Limitations of Current Methods:** Existing Radio Acoustic Sounding Systems (RASS) often suffer from limited height coverage due to the distortion of acoustic wave fronts by temperature gradients and horizontal winds. This misalignment leads to inefficient backscatter and incomplete data, affecting the reliability of atmospheric profiling.
2. **Enhanced Weather Prediction and Climate Research:** Improved height coverage and accuracy in temperature and wind measurements are critical for enhancing weather prediction models and conducting more precise climate research. Better data can lead to more accurate forecasts and a deeper understanding of atmospheric processes.
3. **Technological Advancements:** Advancing the design and optimization of acoustic sources within RASS can significantly reduce the operational costs and improve the scientific capabilities of these systems. This study aims to develop innovative solutions to address the current limitations, making RASS a more effective tool for meteorologists and researchers.
4. **Safety and Preparedness:** Accurate atmospheric profiling is vital for public safety and preparedness in the face of severe weather events. Enhanced measurement techniques can lead to better early warning systems and risk management strategies, thereby protecting lives and property.
5. **Scientific Contributions:** The findings from this study will contribute to the broader field of atmospheric science by providing a more robust method for continuous height coverage. This will facilitate more detailed investigations into the dynamics of the atmosphere and its interactions with various environmental factors.

Given these points, there is a clear and pressing need to optimize the acoustic sources in RASS for improved height coverage and measurement accuracy, thereby advancing both the scientific understanding and practical applications of atmospheric profiling.

This page was intentionally left blank.

# Chapter 2

## Design Methodology

### 2.1 Introduction

In this study, we aimed to optimize the placement of acoustic sources to enhance the performance of a Radio Acoustic Sounding System (RASS) by ensuring maximal coverage and efficient backscatter within the radar antenna array. Here is an overview of the initial methodology employed:

#### 2.1.1 Initial Data Collection

- **Radiosonde Data:** Atmospheric data, including wind and temperature profiles, were collected using radiosondes.

#### 2.1.2 Acoustic Source Placement Strategy

- **Placement on Edges and Corners:** Acoustic sources were placed at strategic locations, including the edges and corners of the radar antenna array, along with a central source.
- **Position Evaluation:** Each position was evaluated to determine the effectiveness in cov-

ering the desired height range and ensuring efficient backscatter within the radar antenna array.

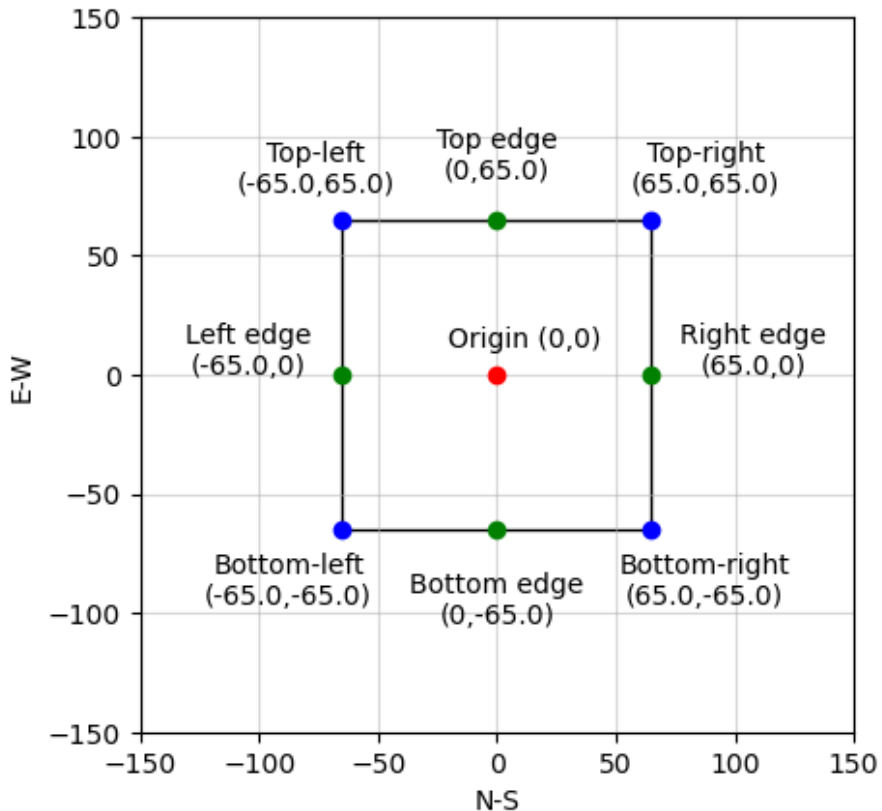
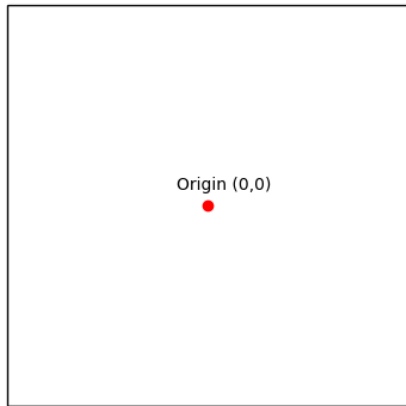


Figure 2.1: Acoustic Source Locations around the antenna array of 130 x130 meters

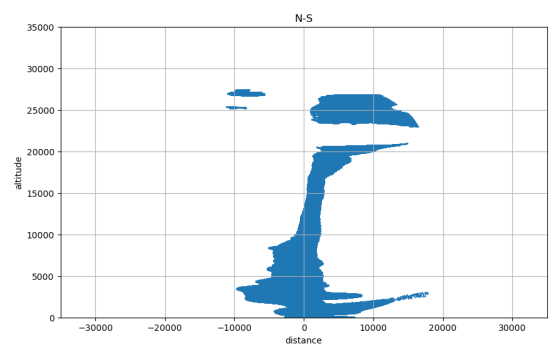
### 2.1.3 Waveform Fitting and Surface Normal Calculation

- **Waveform Fitting:** The atmospheric data waveforms were fitted to a surface model to understand the distribution of the data. Data was filtered and smoothed using a spline interpolation method with tuning parameters such as the smoothing parameter ( $\rho$ ) and grid size.
- **Normal Calculation:** Normals to the fitted surface were calculated to determine the backscattering would land within the radar antenna array. The normals were evaluated to identify those falling within  $\pm 20$  degrees of the radar beam, maximizing coverage within the antenna array.

By systematically evaluating various placements and using data analysis techniques, we aimed to identify the optimal configuration for acoustic sources, thereby improving the efficiency and accuracy of the RASS temperature measurements and checking the improvement in the process.

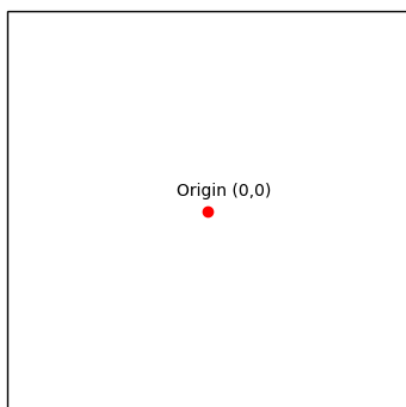


(a)

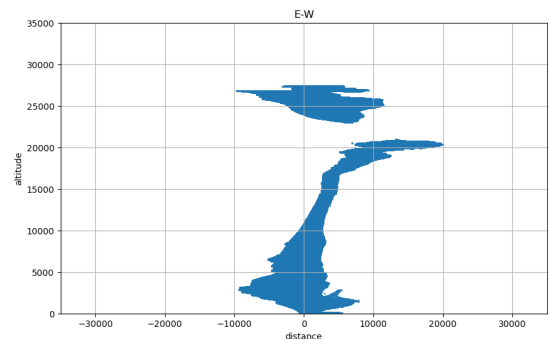


(b)

Figure 2.2: When the source is at the Origin, the portions of acoustic wavefronts in the NS plane from which backscatter would fall on the antenna array



(a)



(b)

Figure 2.3: When the source is at the Origin, the portions of acoustic wavefronts in the EW plane from which backscatter would fall on the antenna array

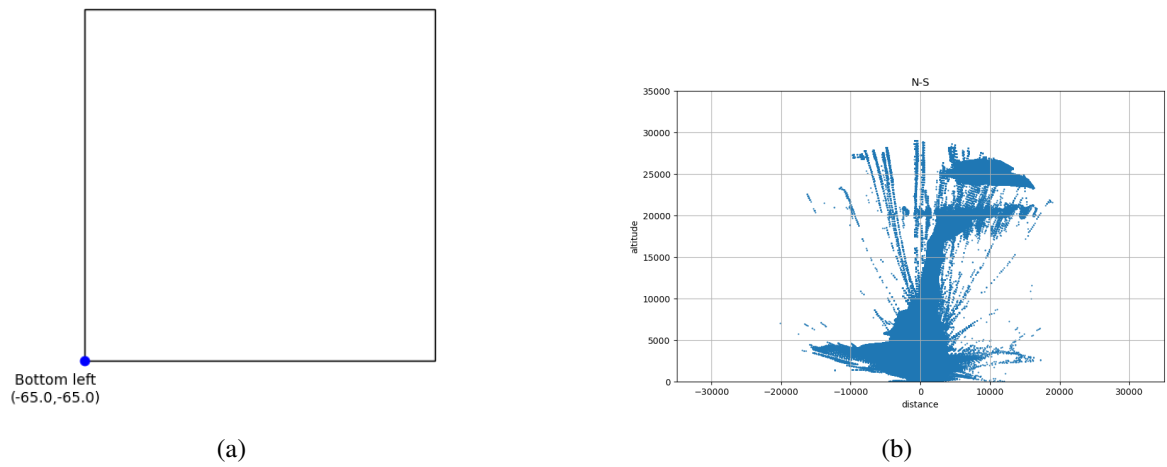


Figure 2.4: When the source is at the Bottom Left corner, the portions of acoustic wavefronts in the NS plane from which backscatter would fall on the antenna array

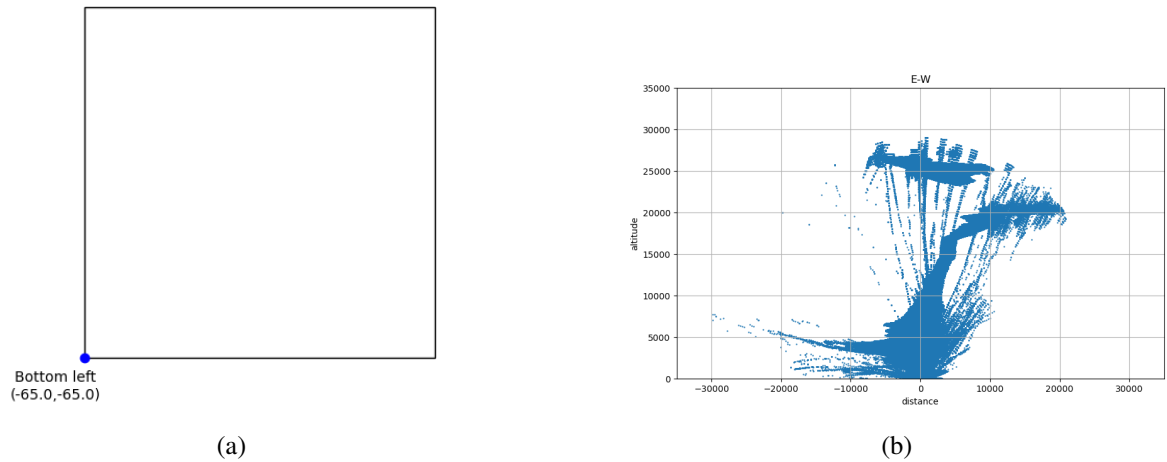
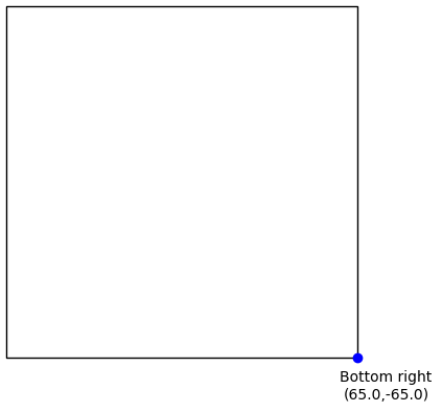
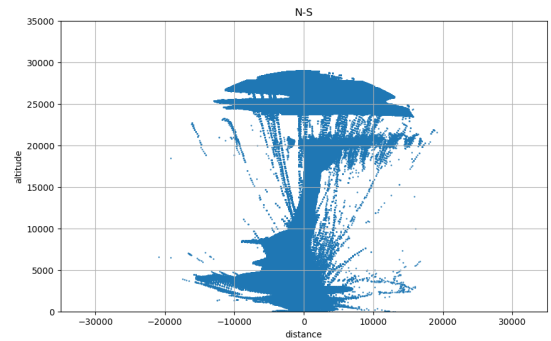


Figure 2.5: When the source is at the Bottom Left corner, the portions of acoustic wavefronts in the EW plane from which backscatter would fall on the antenna array

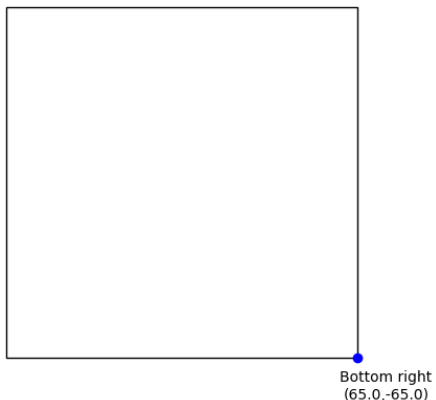


(a)

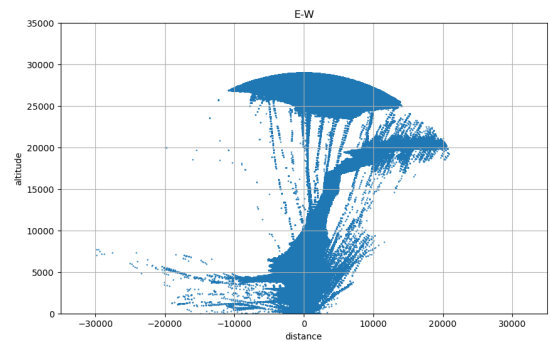


(b)

Figure 2.6: When the source is at the bottom right corner, the portions of acoustic wavefronts in the NS plane from which backscatter would fall on the antenna array



(a)



(b)

Figure 2.7: When the source is at the bottom right corner, the portions of acoustic wavefronts in the EW plane from which backscatter would fall on the antenna array

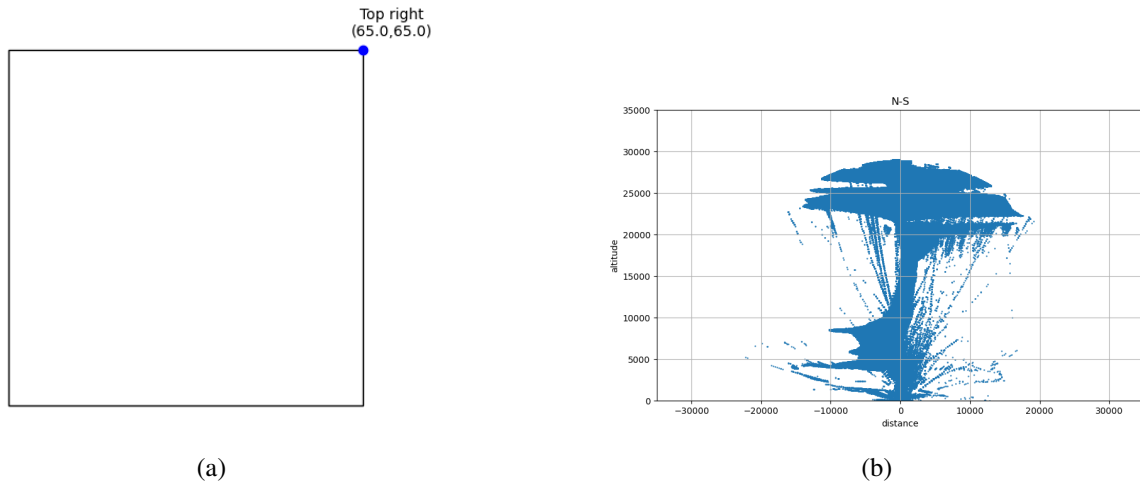


Figure 2.8: When the source is at the top right corner, the portions of acoustic wavefronts in the NS plane from which backscatter would fall on the antenna array

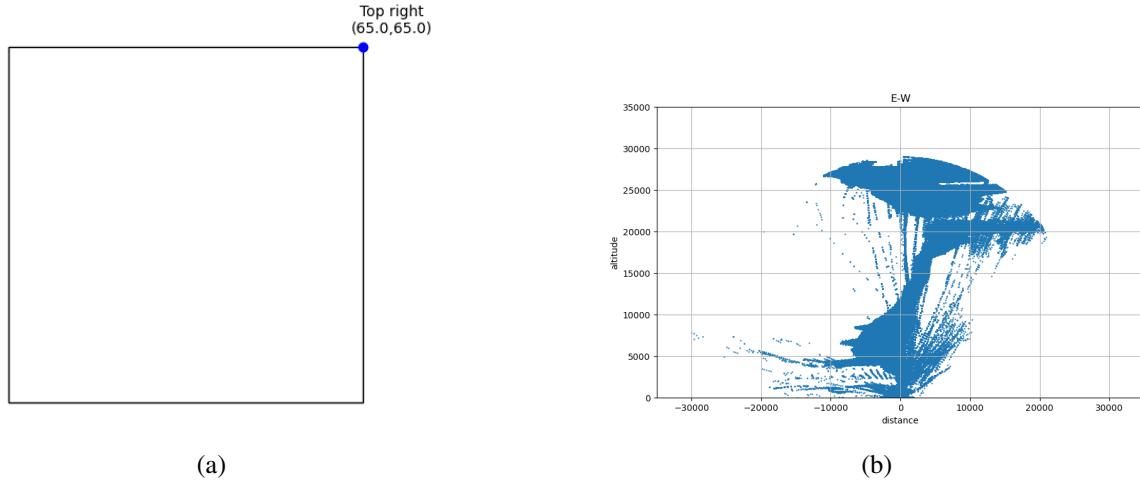
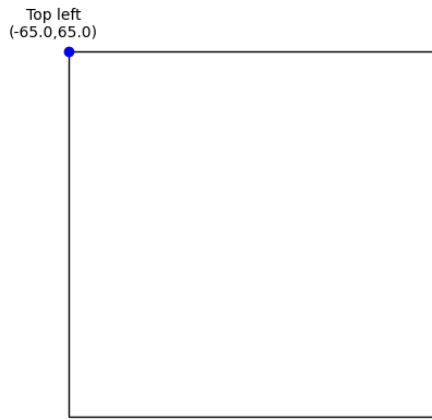
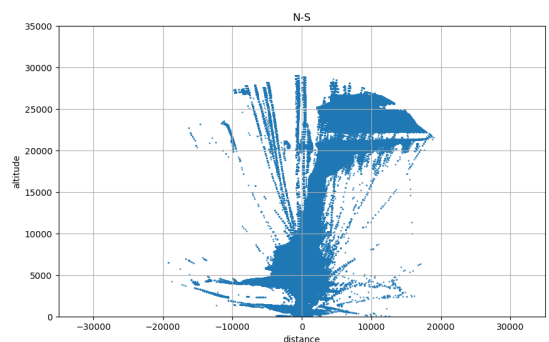


Figure 2.9: When the source is at the top right corner, the portions of acoustic wavefronts in the EW plane from which backscatter would fall on the antenna array

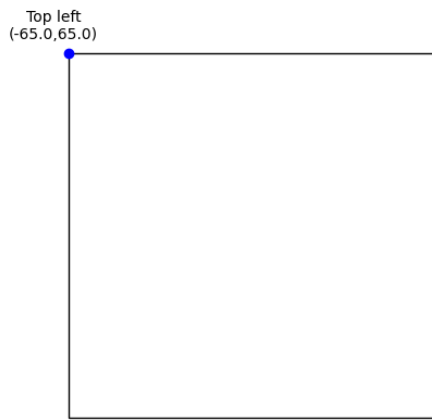


(a)

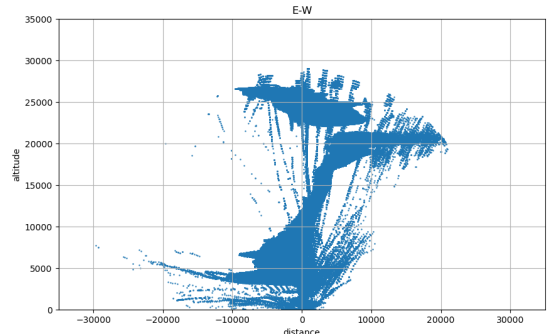


(b)

Figure 2.10: When the source is at the top left corner, the portions of acoustic wavefronts in the NS plane from which backscatter would fall on the antenna array

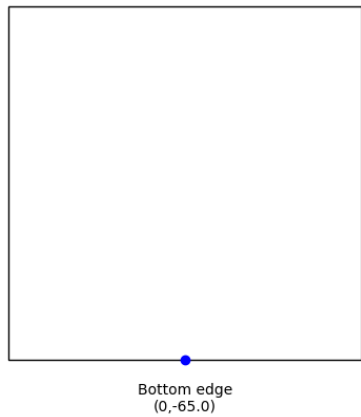


(a)

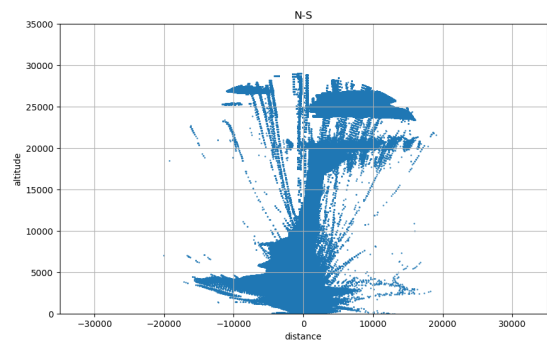


(b)

Figure 2.11: When the source is at the top left corner, the portions of acoustic wavefronts in the EW plane from which backscatter would fall on the antenna array

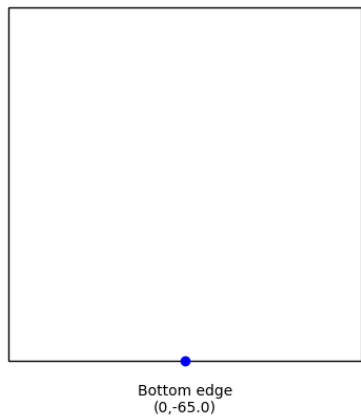


(a)

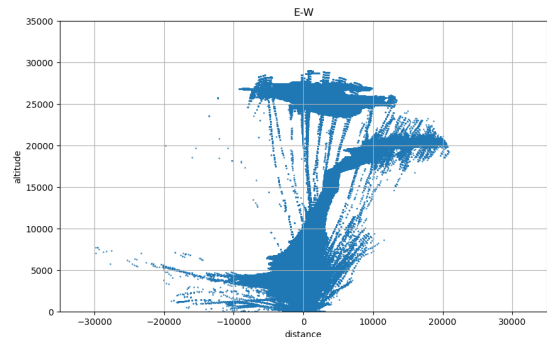


(b)

Figure 2.12: When the source is at the bottom edge, the portions of acoustic wavefronts in the NS plane from which backscatter would fall on the antenna array

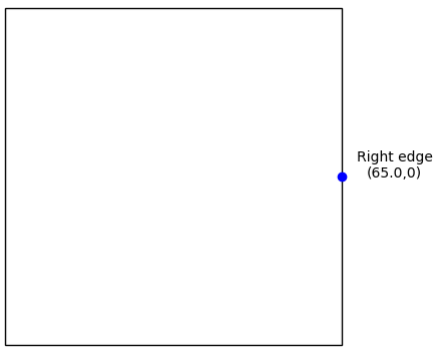


(a)

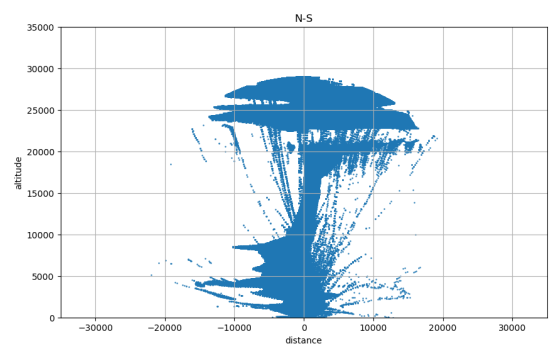


(b)

Figure 2.13: When the source is at the bottom edge, the portions of acoustic wavefronts in the EW plane from which backscatter would fall on the antenna array

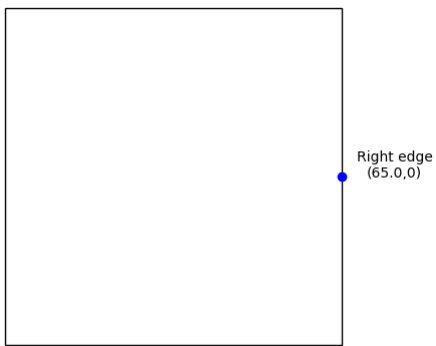


(a)

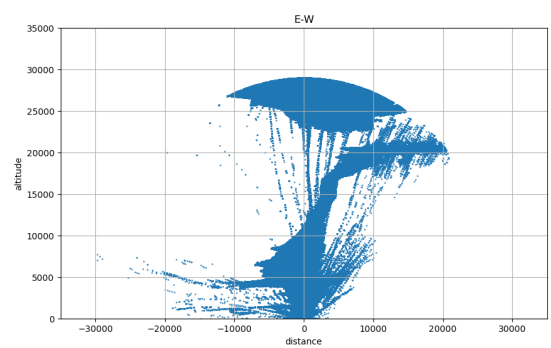


(b)

Figure 2.14: When the source is at the right edge, the portions of acoustic wavefronts in the NS plane from which backscatter would fall on the antenna array



(a)



(b)

Figure 2.15: When the source is at the right edge, the portions of acoustic wavefronts in the EW plane from which backscatter would fall on the antenna array

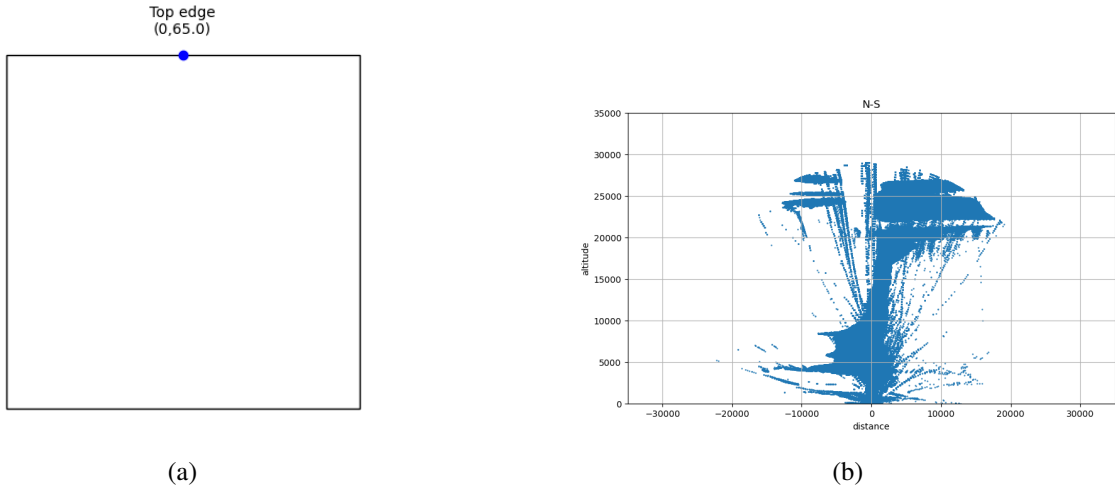


Figure 2.16: When the source is at the top edge, the portions of acoustic wavefronts in the NS plane from which backscatter would fall on the antenna array

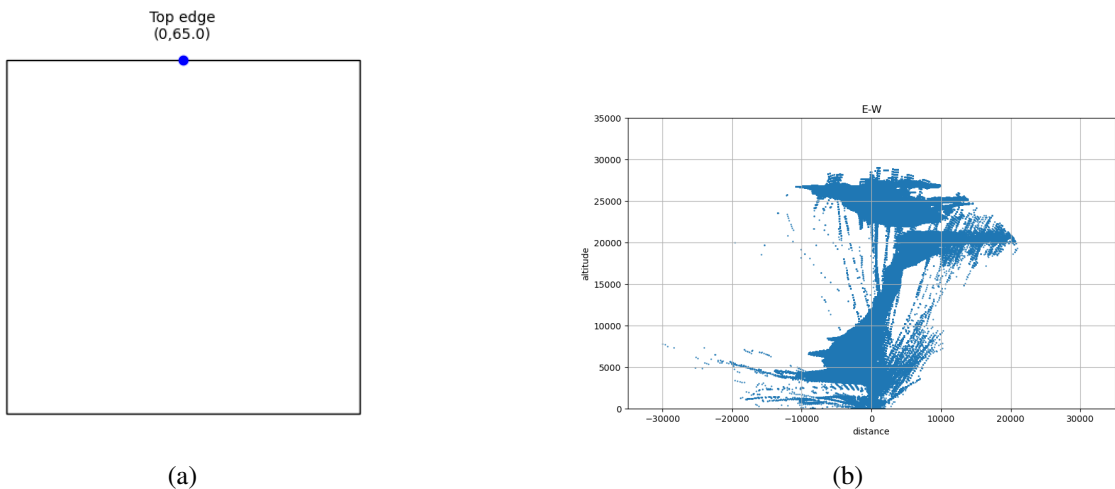
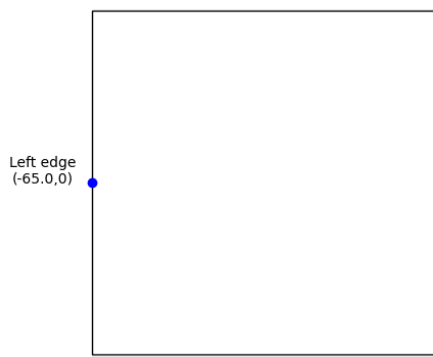
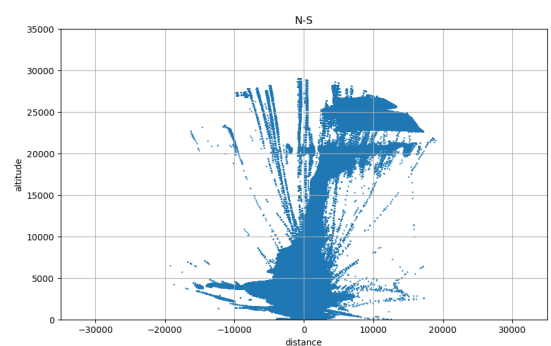


Figure 2.17: When the source is at the top edge, the portions of acoustic wavefronts in the EW plane from which backscatter would fall on the antenna array

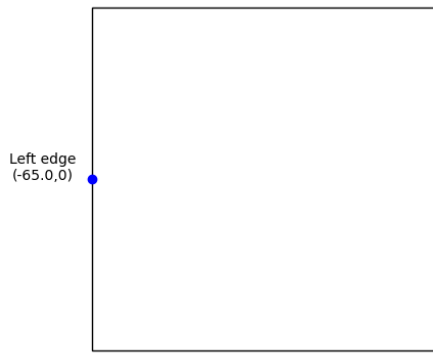


(a)

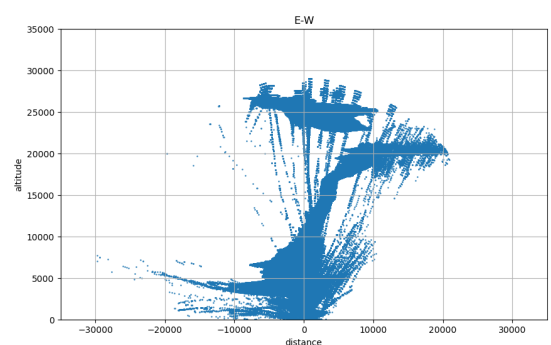


(b)

Figure 2.18: When the source is at the left edge, the portions of acoustic wavefronts in the NS plane from which backscatter would fall on the antenna array



(a)



(b)

Figure 2.19: When the source is at the left edge, the portions of acoustic wavefronts in the EW plane from which backscatter would fall on the antenna array

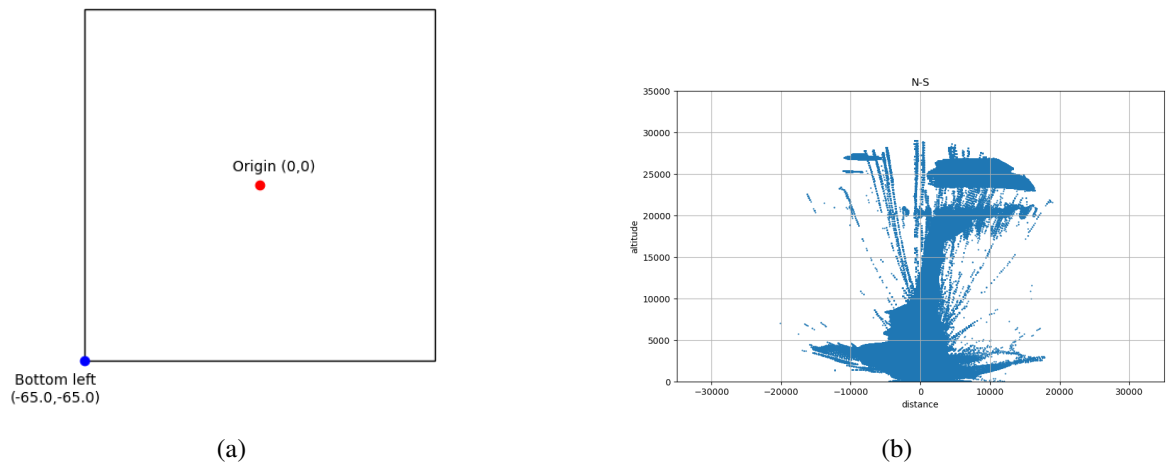


Figure 2.20: When the sources are at the origin and bottom left corner, the portions of acoustic wavefronts in the NS plane from which backscatter would fall on the antenna array

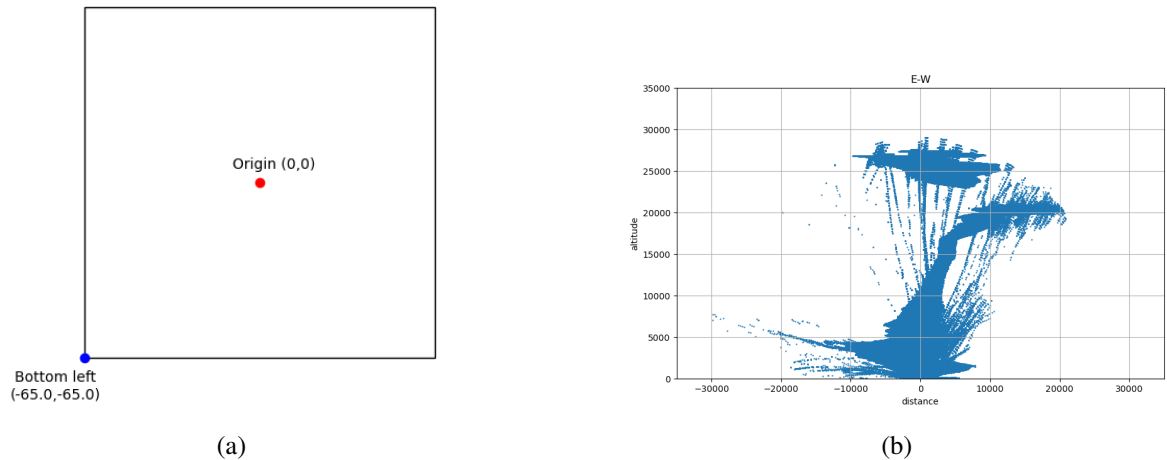


Figure 2.21: When the source is at the origin and bottom left corner, the portions of acoustic wavefronts in the EW plane from which backscatter would fall on the antenna array

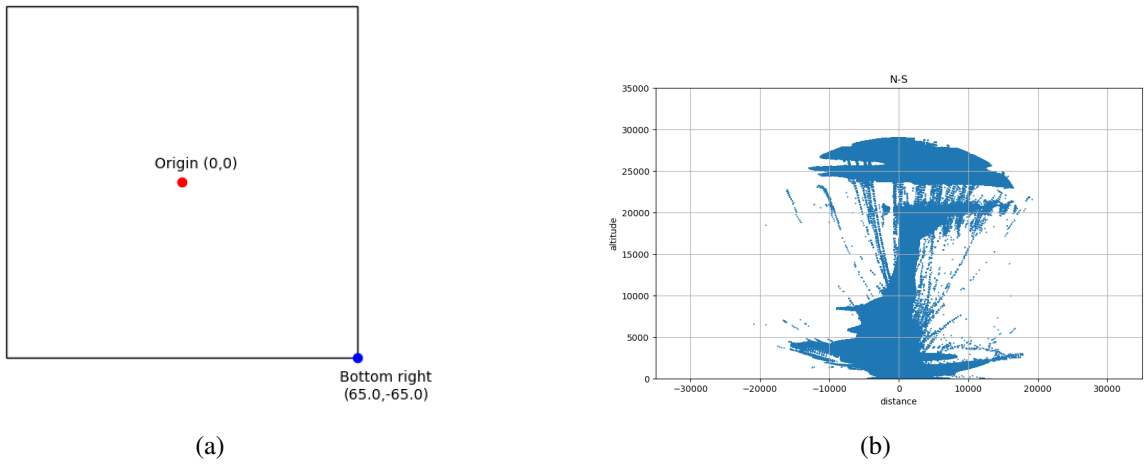


Figure 2.22: When the sources are at the origin and bottom right corner, the portions of acoustic wavefronts in the NS plane from which backscatter would fall on the antenna array

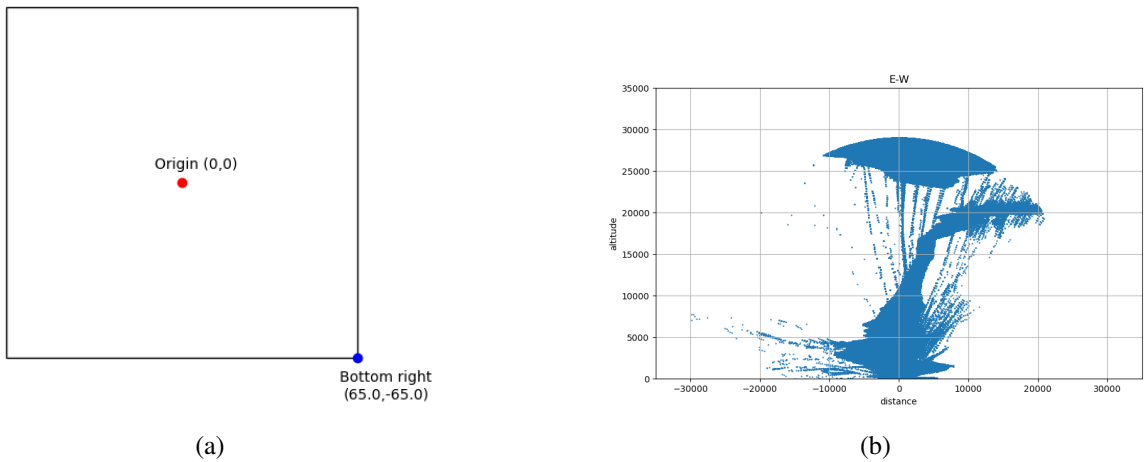


Figure 2.23: When the source is at the origin and bottom right corner, the portions of acoustic wavefronts in the EW plane from which backscatter would fall on the antenna array

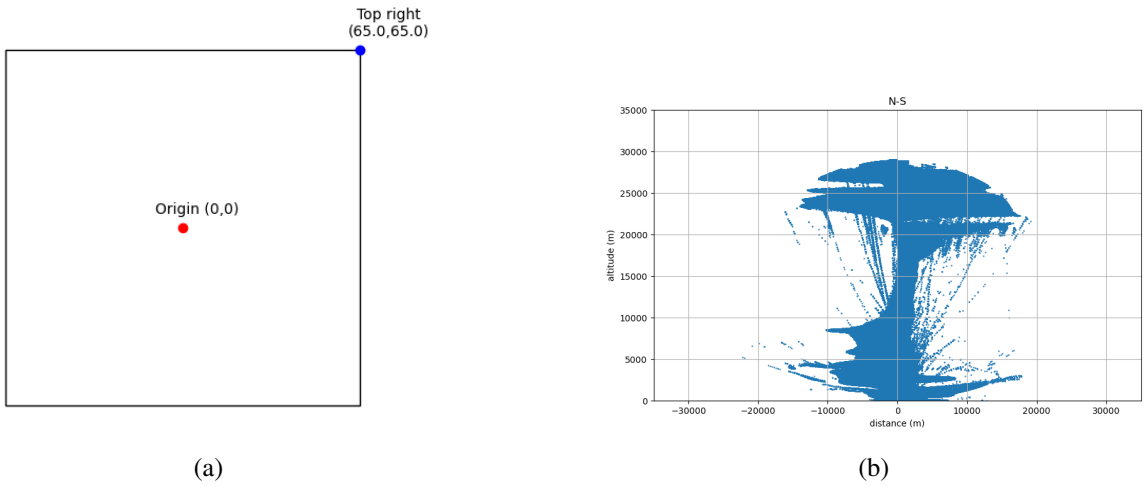


Figure 2.24: When the sources are at the origin and top right corner, the portions of acoustic wavefronts in the NS plane from which backscatter would fall on the antenna array

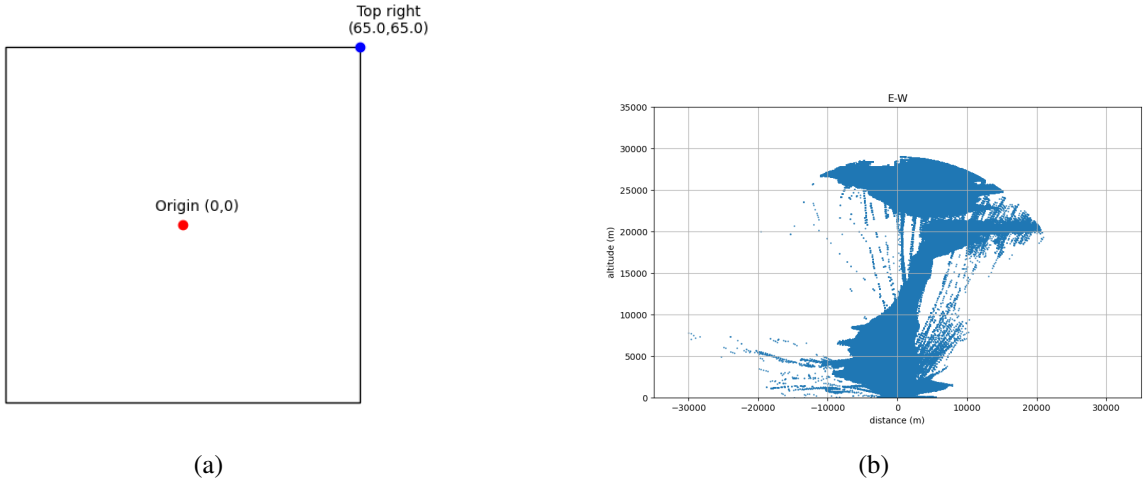
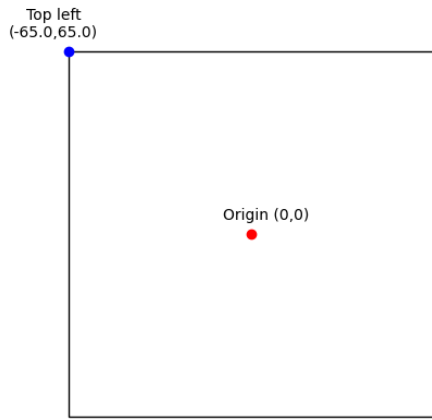
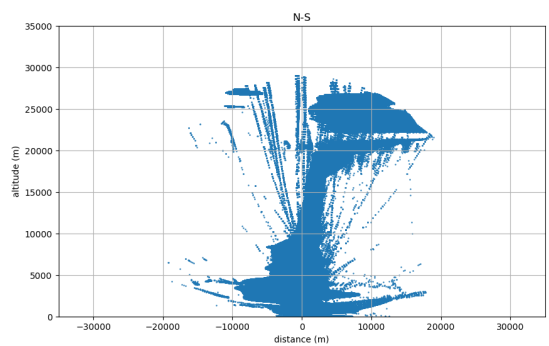


Figure 2.25: When the source is at the origin and top right corner, the portions of acoustic wavefronts in the EW plane from which backscatter would fall on the antenna array

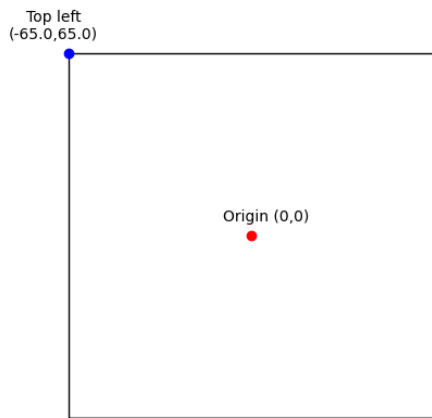


(a)

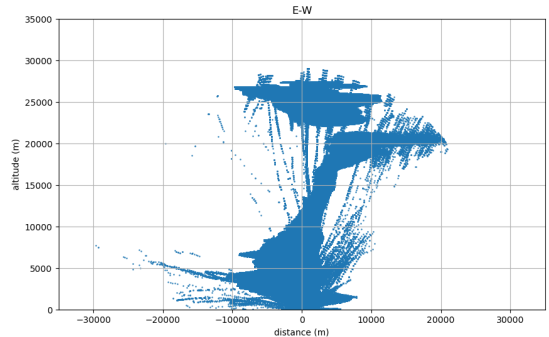


(b)

Figure 2.26: When the sources are at the origin and top left corner, the portions of acoustic wavefronts in the NS plane from which backscatter would fall on the antenna array



(a)



(b)

Figure 2.27: When the source is at the origin and top left corner, the portions of acoustic wavefronts in the EW plane from which backscatter would fall on the antenna array

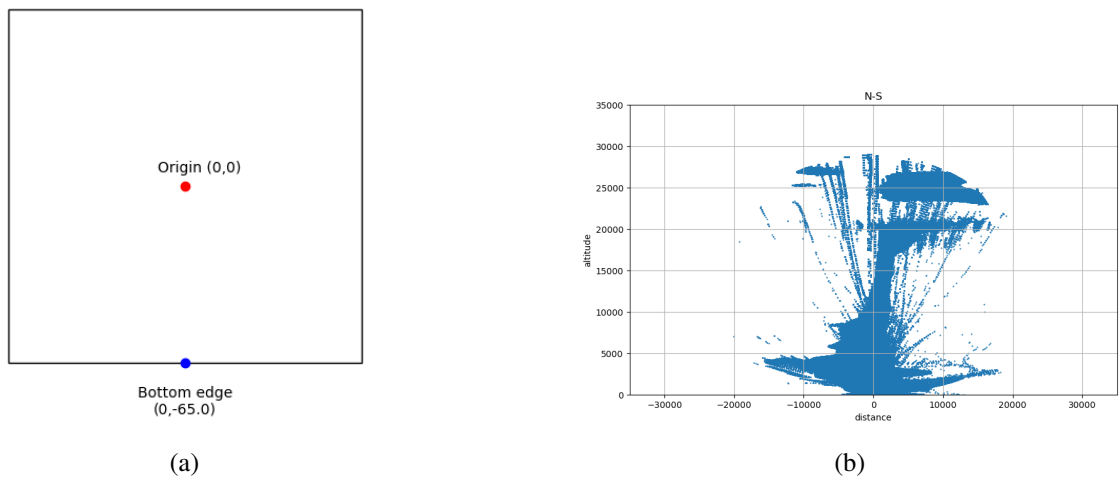


Figure 2.28: When the sources are at the origin and bottom edge, the portions of acoustic wavefronts in the NS plane from which backscatter would fall on the antenna array

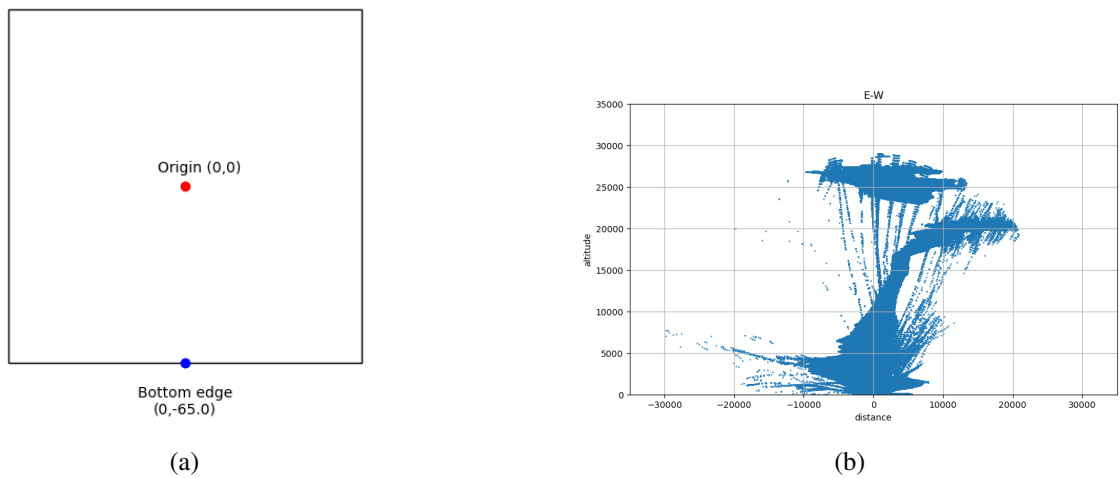


Figure 2.29: When the source is at the origin and bottom edge, the portions of acoustic wavefronts in the EW plane from which backscatter would fall on the antenna array

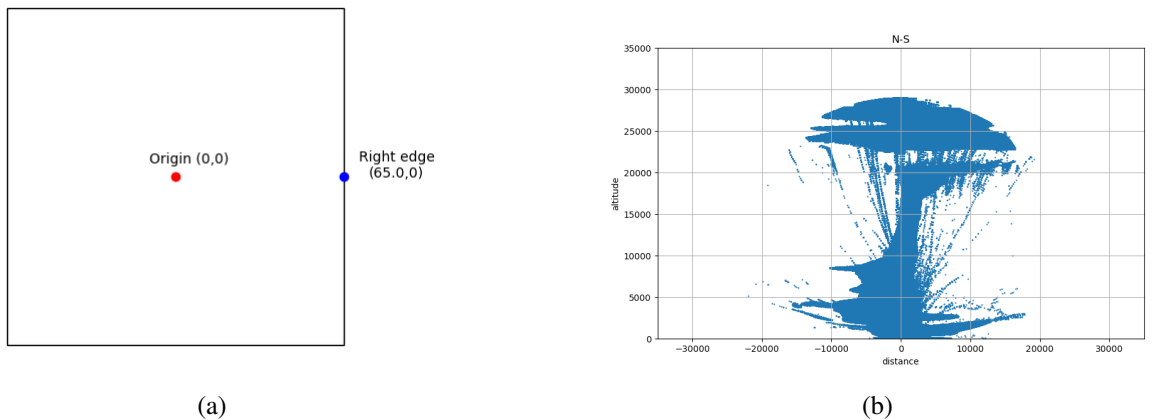


Figure 2.30: When the sources are at the origin and right edge, the portions of acoustic wavefronts in the NS plane from which backscatter would fall on the antenna array

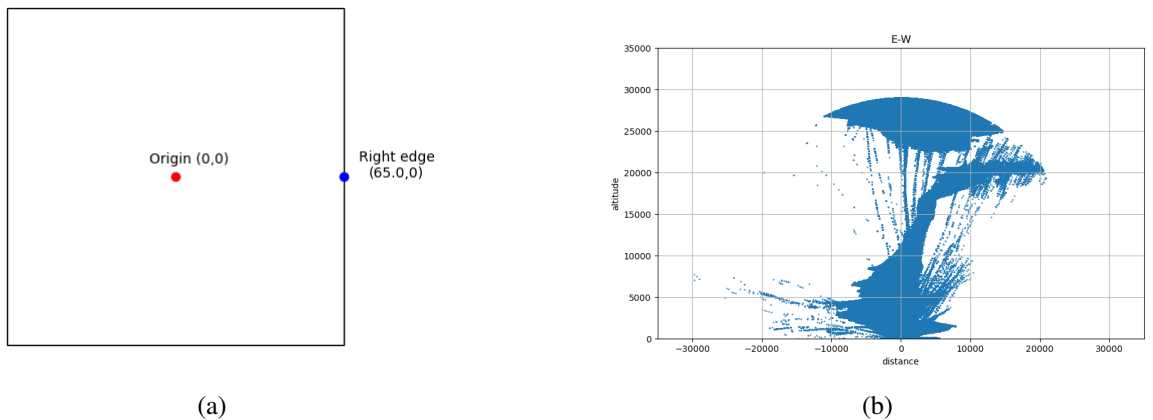
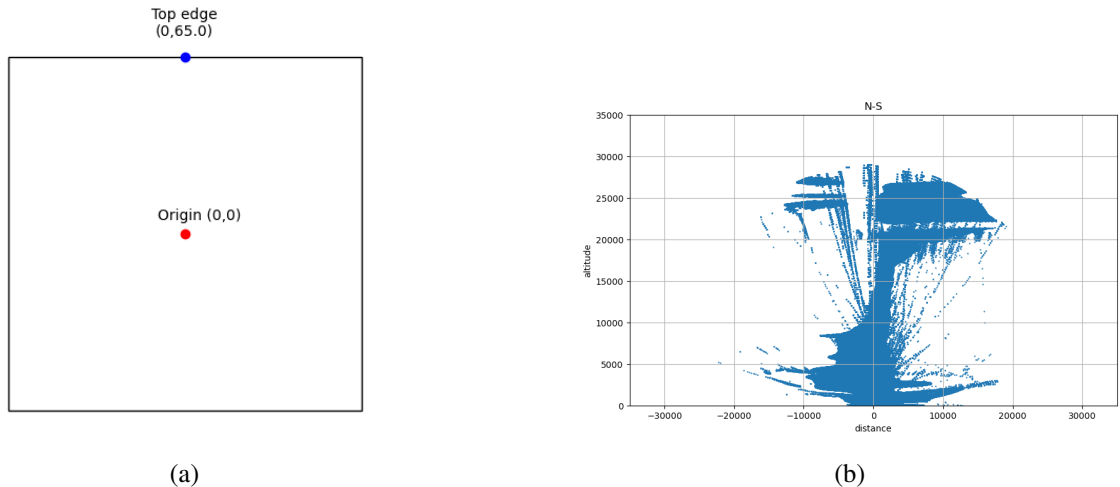


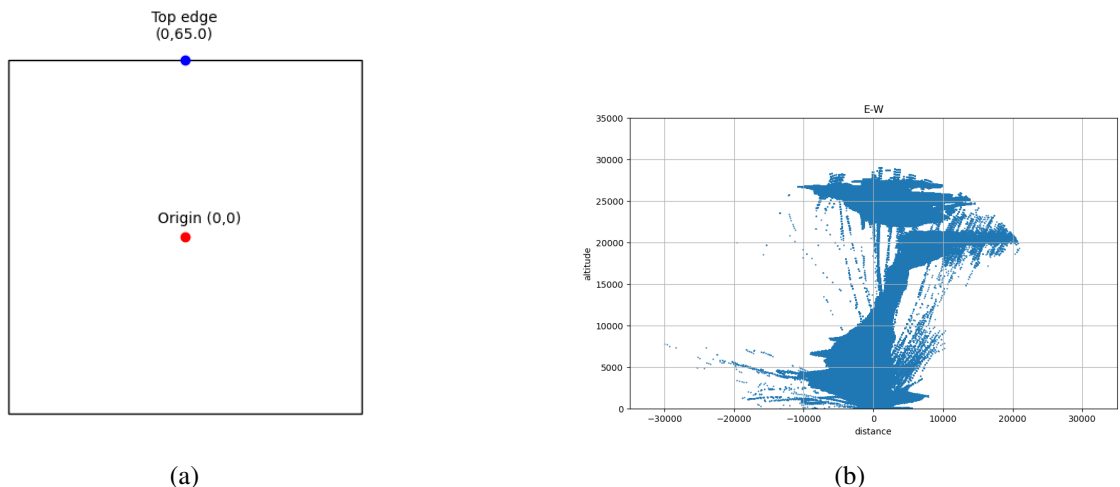
Figure 2.31: When the source is at the origin and right edge, the portions of acoustic wavefronts in the EW plane from which backscatter would fall on the antenna array



(a)

(b)

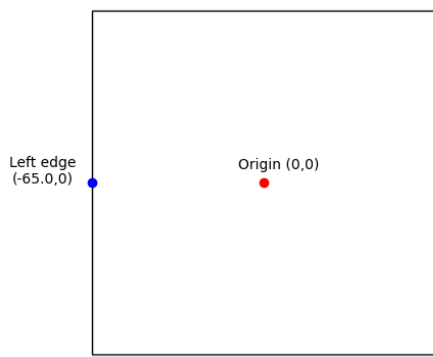
Figure 2.32: When the sources are at the origin and top edge, the portions of acoustic wavefronts in the NS plane from which backscatter would fall on the antenna array



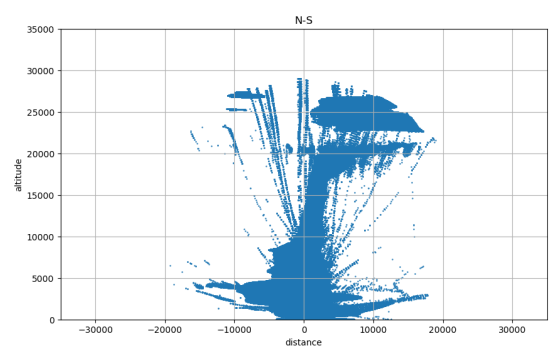
(a)

(b)

Figure 2.33: When the source is at the origin and top edge, the portions of acoustic wavefronts in the EW plane from which backscatter would fall on the antenna array

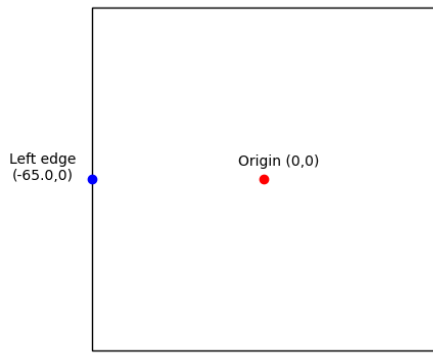


(a)

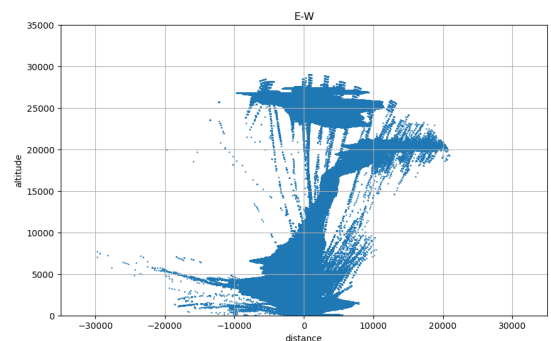


(b)

Figure 2.34: When the sources are at the origin and left edge, the portions of acoustic wavefronts in the NS plane from which backscatter would fall on the antenna array



(a)



(b)

Figure 2.35: When the source is at the origin and left edge, the portions of acoustic wavefronts in the EW plane from which backscatter would fall on the antenna array

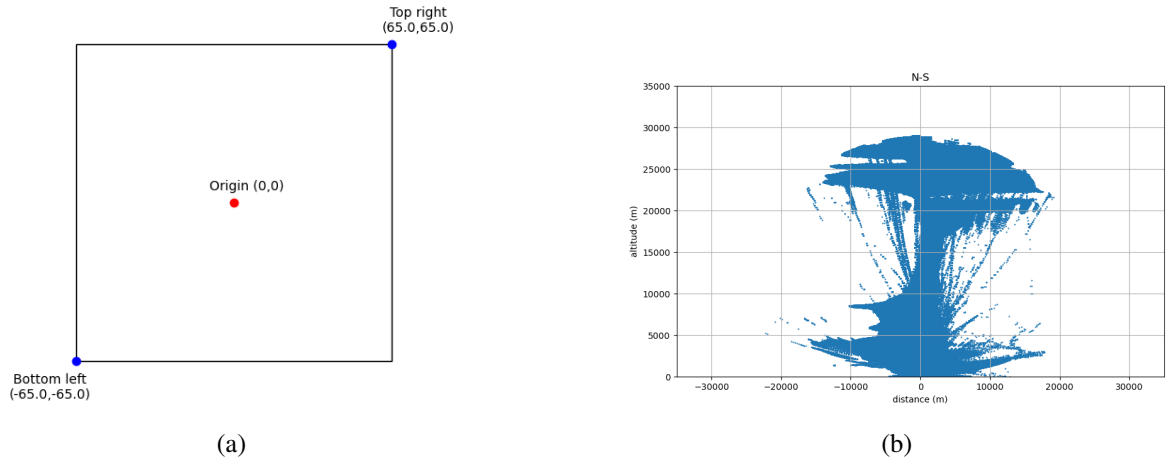


Figure 2.36: When the sources are at the origin, bottom left corner, and top right corner, the portions of acoustic wavefronts in the NS plane from which backscatter would fall on the antenna array

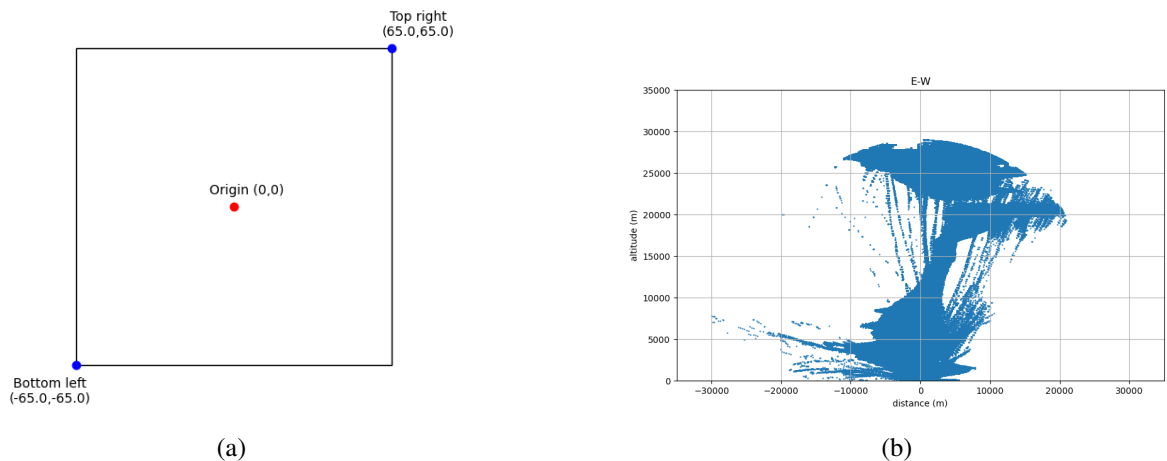
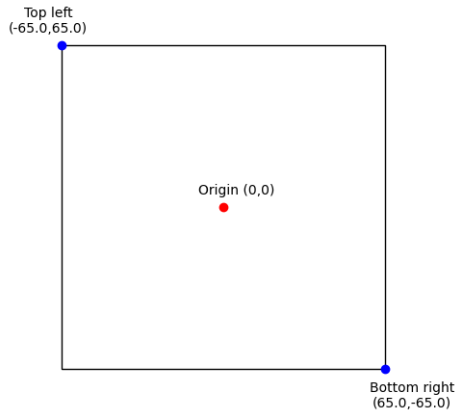
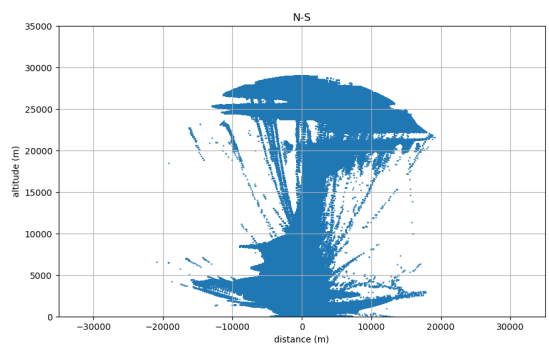


Figure 2.37: When the source is at the origin, bottom left corner, and top right corner, the portions of acoustic wavefronts in the EW plane from which backscatter would fall on the antenna array

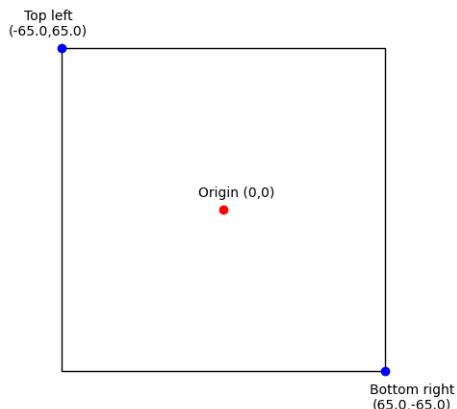


(a)

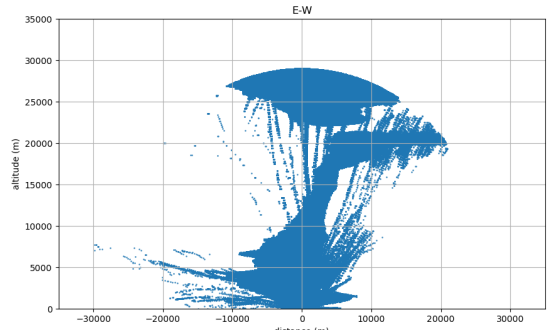


(b)

Figure 2.38: When the sources are at the origin, bottom right corner, and top left corner, the portions of acoustic wavefronts in the NS plane from which backscatter would fall on the antenna array



(a)



(b)

Figure 2.39: When the source is at the origin, bottom right corner, and top left corner, the portions of acoustic wavefronts in the EW plane from which backscatter would fall on the antenna array

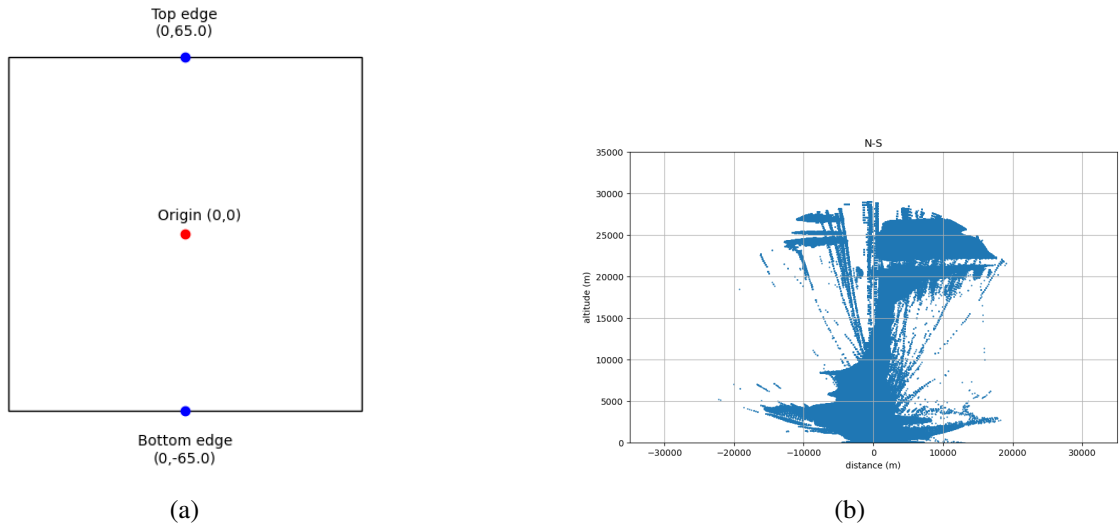


Figure 2.40: When the sources are at the origin, bottom edge, and top edge, the portions of acoustic wavefronts in the NS plane from which backscatter would fall on the antenna array

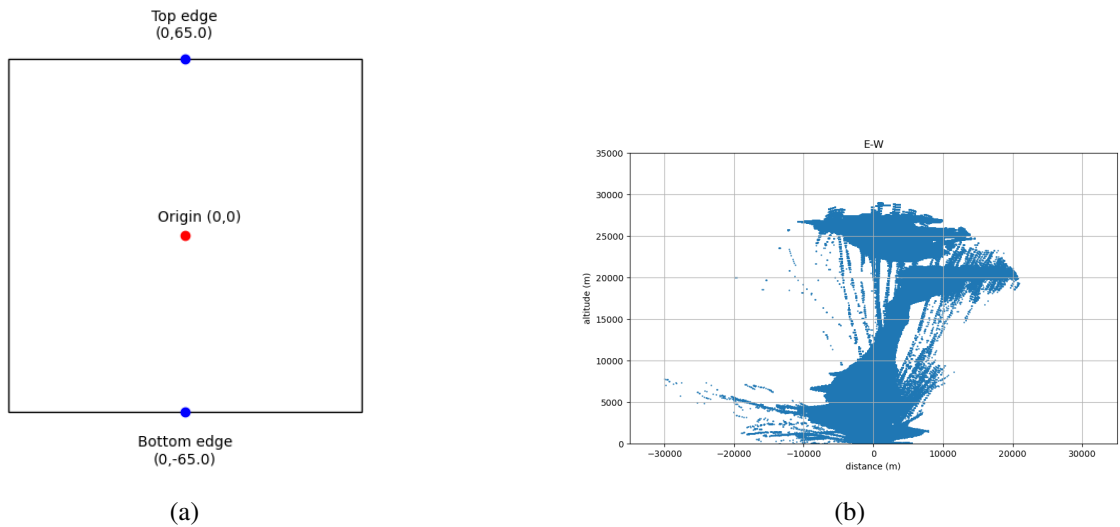


Figure 2.41: When the source is at the origin, bottom edge, and top edge, the portions of acoustic wavefronts in the EW plane from which backscatter would fall on the antenna array

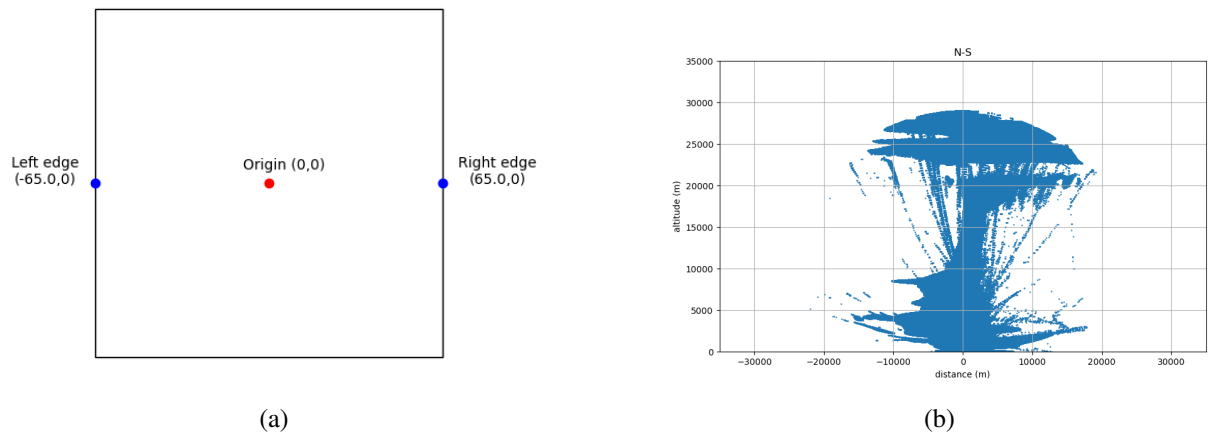


Figure 2.42: When the sources are at the origin, right edge, and left edge, the portions of acoustic wavefronts in the NS plane from which backscatter would fall on the antenna array

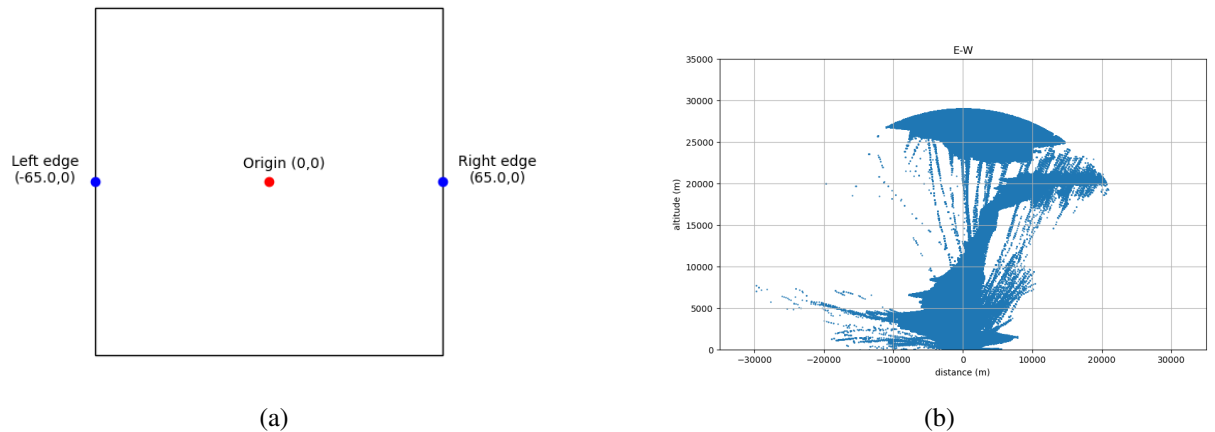


Figure 2.43: When the source is at the origin, right edge, and left edge, the portions of acoustic wavefronts in the EW plane from which backscatter would fall on the antenna array

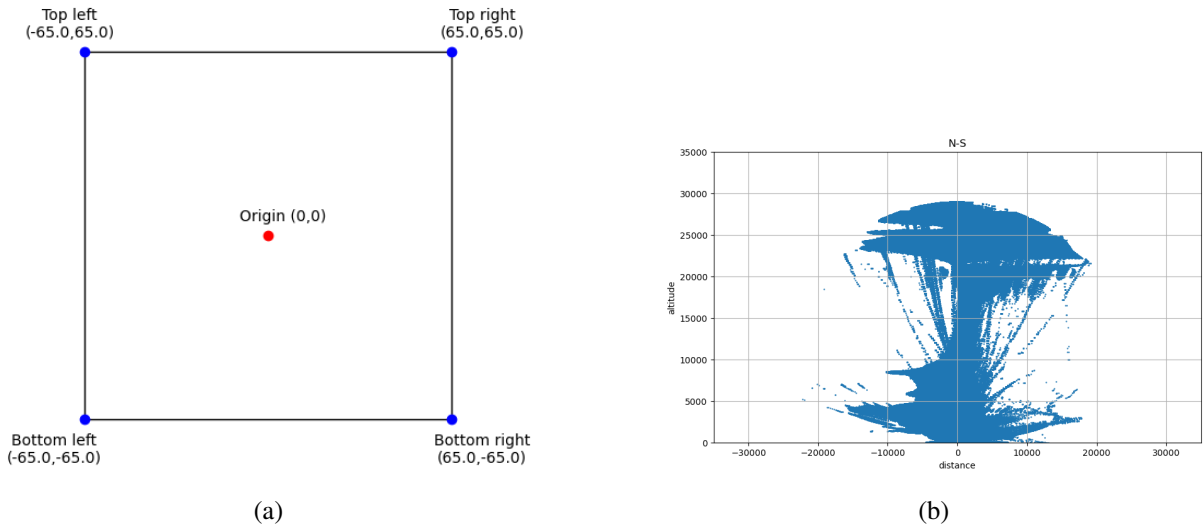


Figure 2.44: When the sources are at the origin and all the corners, the portions of acoustic wavefronts in the NS plane from which backscatter would fall on the antenna array

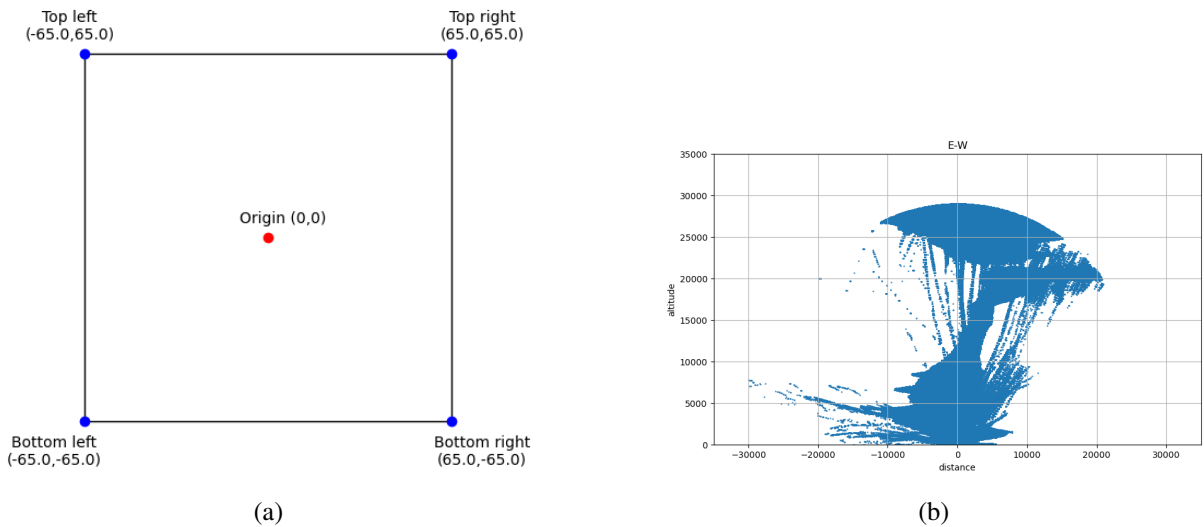
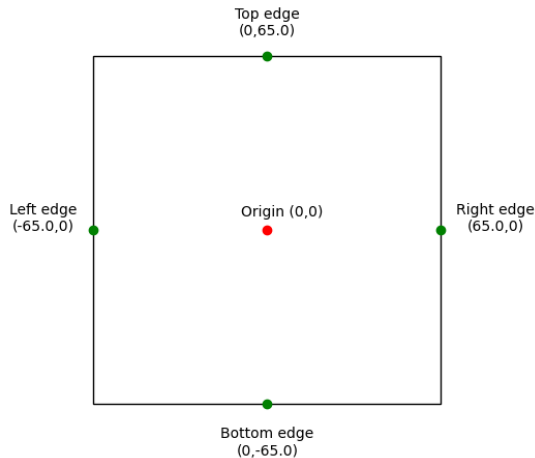
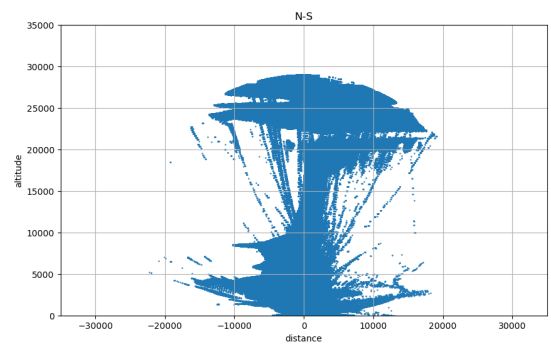


Figure 2.45: When the source is at the origin, and all the corners, the portions of acoustic wavefronts in the EW plane from which backscatter would fall on the antenna array

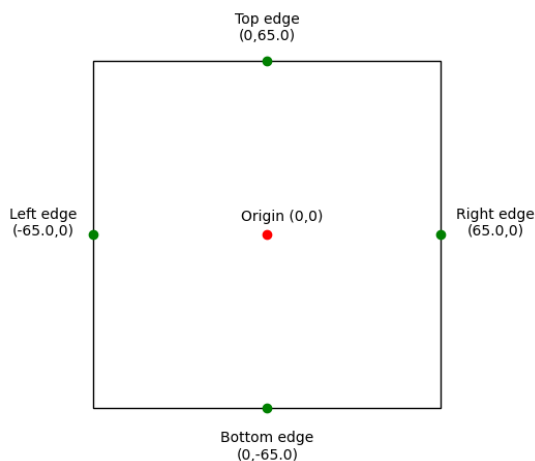


(a)

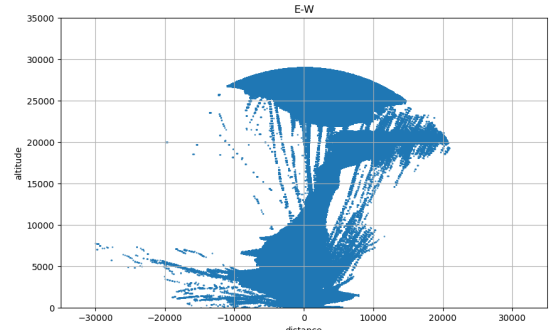


(b)

Figure 2.46: When the sources are at the origin, and all the edges, the portions of acoustic wavefronts in the NS plane from which backscatter would fall on the antenna array



(a)



(b)

Figure 2.47: When the source is at the origin, and all the edges, the portions of acoustic wavefronts in the EW plane from which backscatter would fall on the antenna array

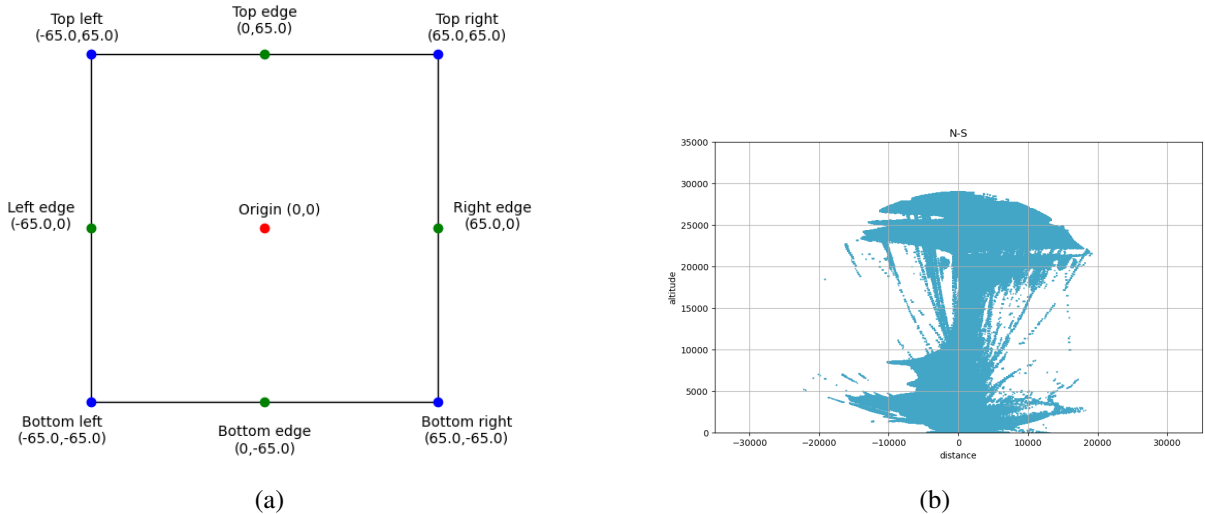


Figure 2.48: When the sources are at the origin, all corners and edges, the portions of acoustic wavefronts in the NS plane from which backscatter would fall on the antenna array

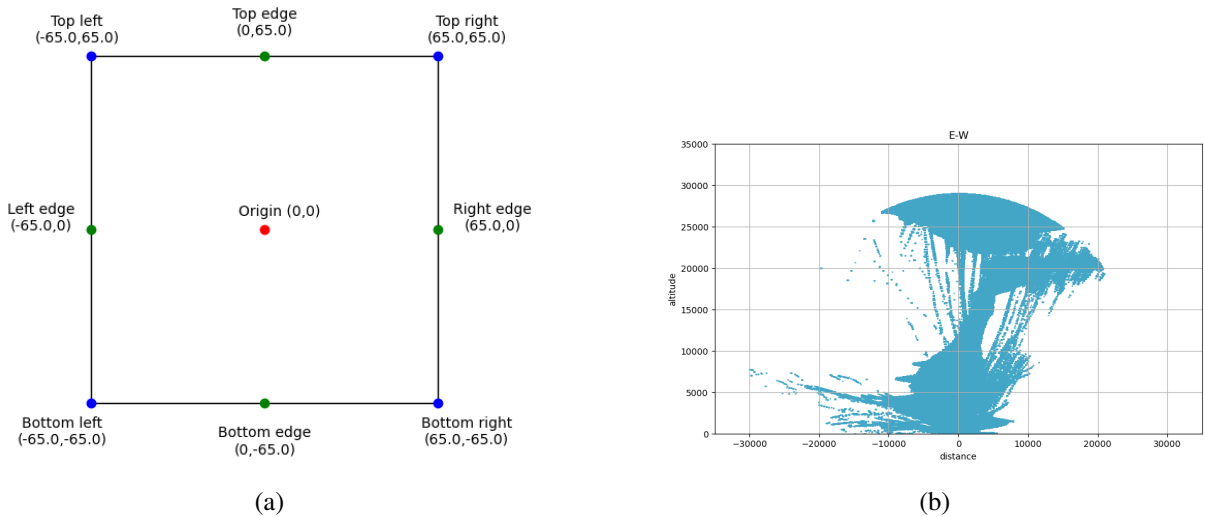


Figure 2.49: When the source is at the origin, all corners and edges, the portions of acoustic wavefronts in the EW plane from which backscatter would fall on the antenna array

### **2.1.4 Effectiveness of this approach:**

The results of our study demonstrate that strategic placement and optimization of acoustic sources did enhance the performance of the RASS. By ensuring continuous backscattering with respect to height and adding more acoustic sources, we can achieve better height coverage and more accurate atmospheric temperature measurements. The combination of data analysis techniques and systematic evaluation of acoustic source positions has proven to be a robust approach for improving RASS efficiency and accuracy.

Instead of brute-forcing every possible position, a more efficient method involves analyzing where the backscattering normals intersect the ground. By identifying these points, we can strategically place the acoustic sources to maximize improvement in height coverage and measurement accuracy. This targeted approach allows us to optimize the source positions more effectively and efficiently.

## **2.2 Design Principles**

### **1. Data-Driven Approach:**

- Leverage atmospheric data from radiosonde measurements to guide the design and optimization of acoustic source placements, ensuring strategic positioning based on real-world atmospheric conditions.

### **2. Surface Fitting and Normal Calculation:**

- Utilize surface fitting techniques to model atmospheric waveforms and calculate normals, enabling precise identification of potential acoustic source locations that align with the optimal sensing range of the antenna array.

### **3. Optimization through Sliding Window Technique:**

- Implement a sliding window method to systematically evaluate and select acoustic source locations that maximize point coverage on the surface, optimizing source placement for enhanced measurement reliability and accuracy.

### **4. Clustering for Simplification:**

- Use clustering algorithms to reduce the number of potential acoustic source locations while maintaining maximum coverage, improving operational efficiency and simplifying the deployment and management of acoustic sources.

### **5. Maximization of Coverage and Alignment:**

- Optimize the placement of acoustic sources to maximize coverage within the antenna array and ensure alignment with radar wave vectors, enhancing the efficiency of backscatter detection and the quality of temperature and wind profiles.

## **6. Iterative Improvement:**

- Continuously refine acoustic source placement strategies through iterative feedback and results, enabling ongoing improvements in height coverage and measurement precision for atmospheric profiling.

These design principles outline a systematic, data-driven approach to optimizing acoustic sources in RASS, focusing on maximizing measurement and coverage effectiveness and operational efficiency.

## 2.3 Flowchart

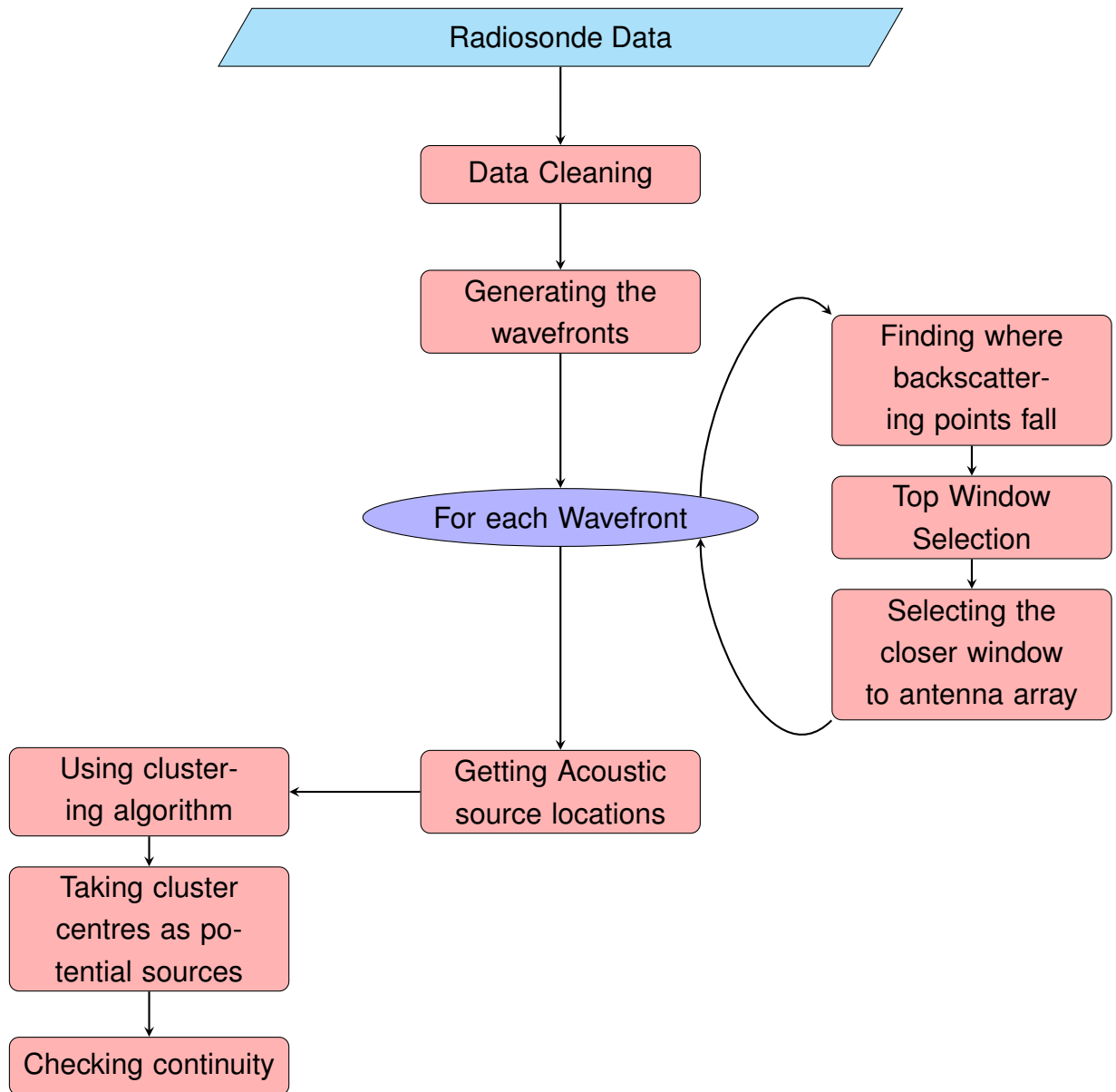
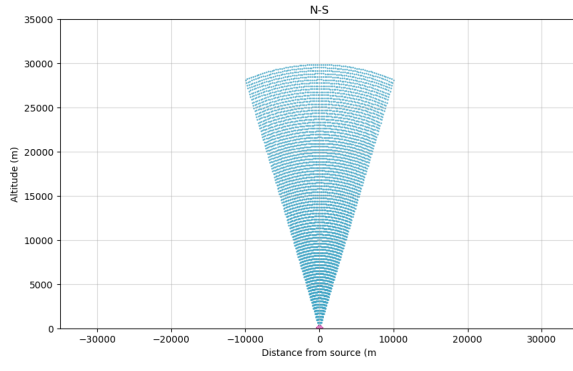


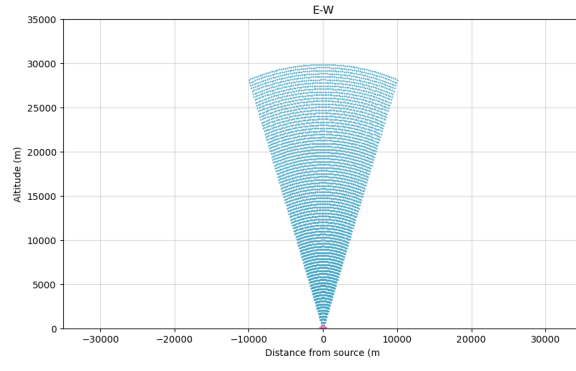
Figure 2.50: Flowchart of the Design

## 2.4 Design Implementation

The backscatter from the acoustic sound source at the origin is in the range of -20 to +20 degrees in an ideal scenario



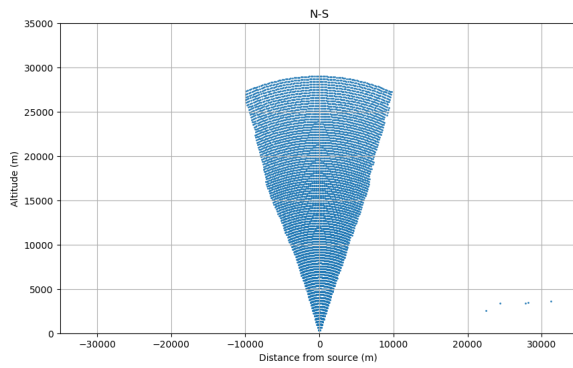
(a)



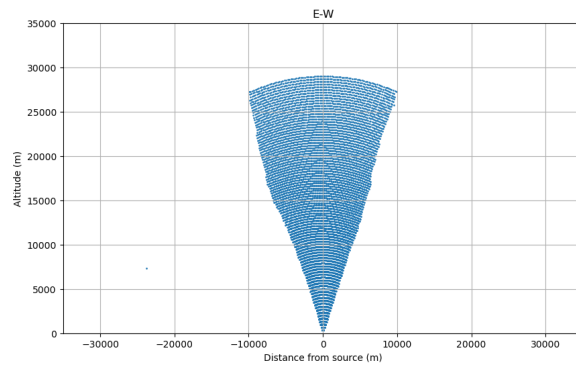
(b)

Figure 2.51

The backscatter from the acoustic sound source at the origin is in the range of -20 to +20 degrees. Here is the measured temperature and wind from the radiosonde flight of 03 Dec 2007.



(a)



(b)

Figure 2.52

Now the backscatter falls within the antenna array and has the normal angle in between -20 to +20 degrees.

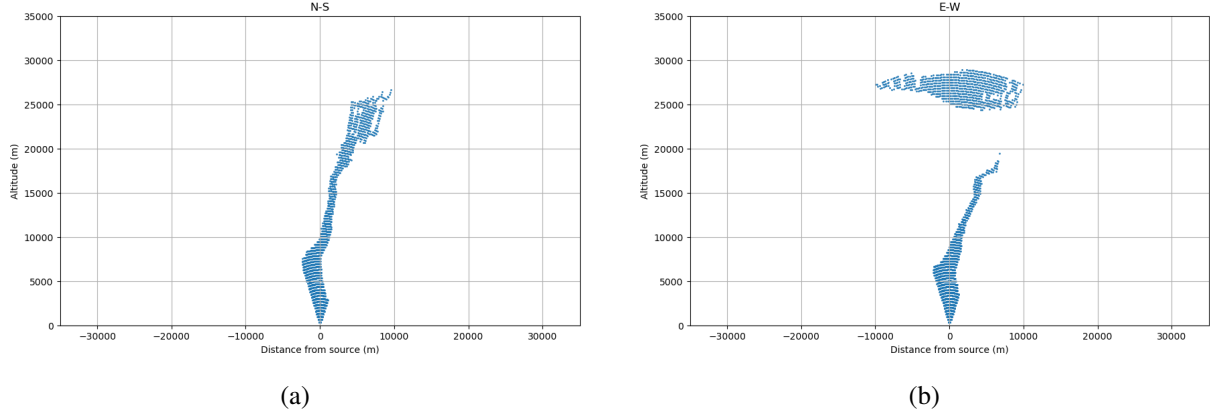


Figure 2.53

The picture shows a combination of two elements: the blue area represents the maximum coverage of the antenna array. In contrast, the red area indicates where the backscatter falls within this coverage.

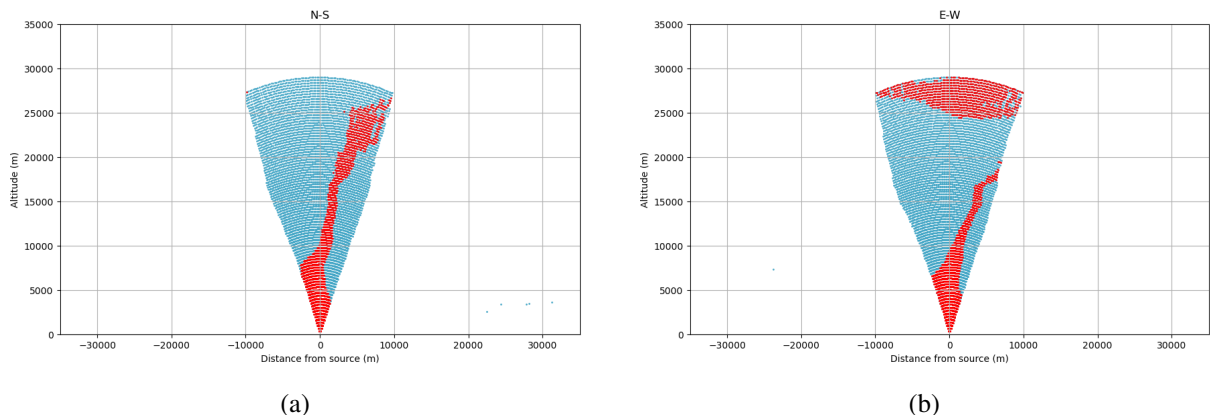


Figure 2.54

Now by taking one wavefront and checking where all the normals are falling on the ground.

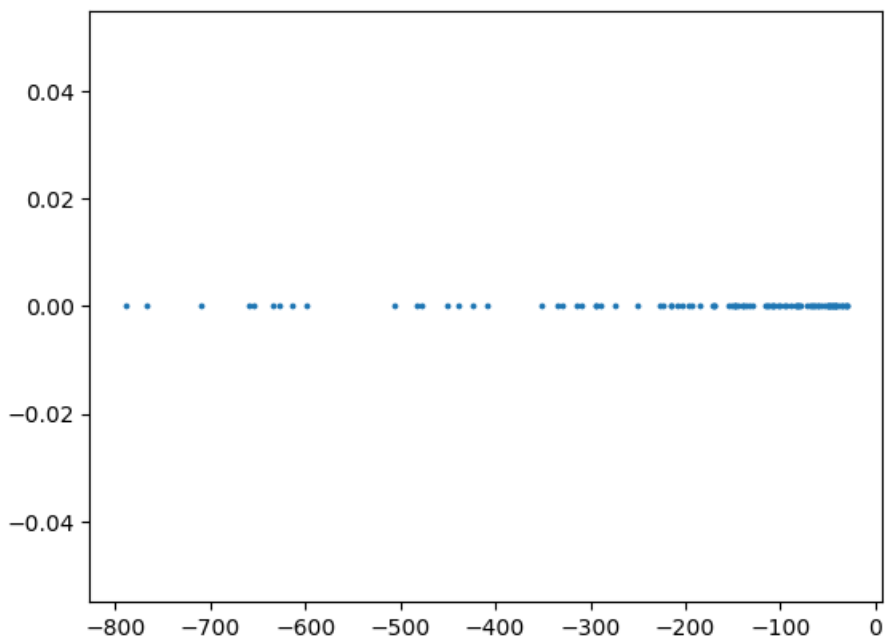


Figure 2.55

We can observe that clusters are forming. By taking a window of 130m, which corresponds to the dimension of the antenna array, we can check for each point to see which one has the highest number of points inside the window. The acoustic source can then be moved to that location. The graph below shows the arrangement before adjustment (at origin) and after adjustment to the location with the maximum points within the window. We can see that the coverage has increased.

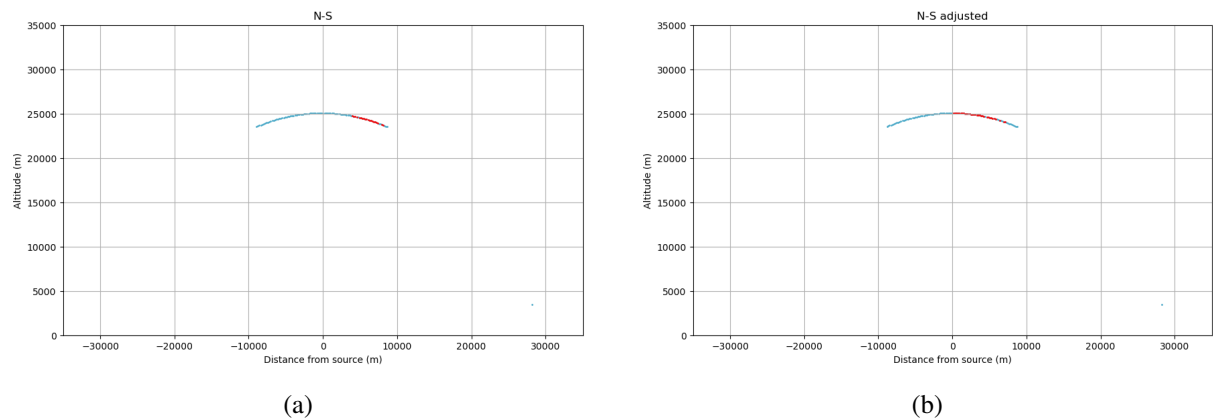


Figure 2.56: showed in the N-S plane

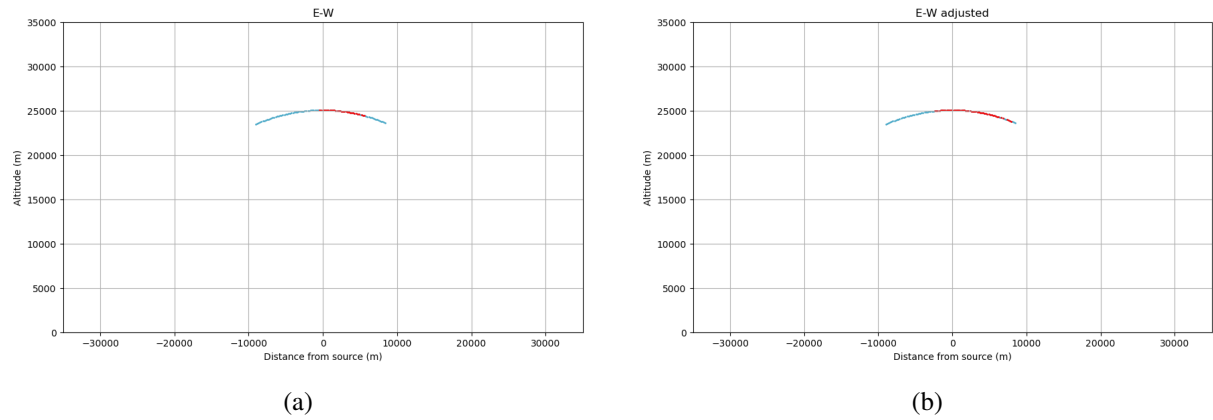


Figure 2.57: showed in the E-W plane

By maximizing the number of points falling inside the antenna array for every wavefront, we obtain the following graphs

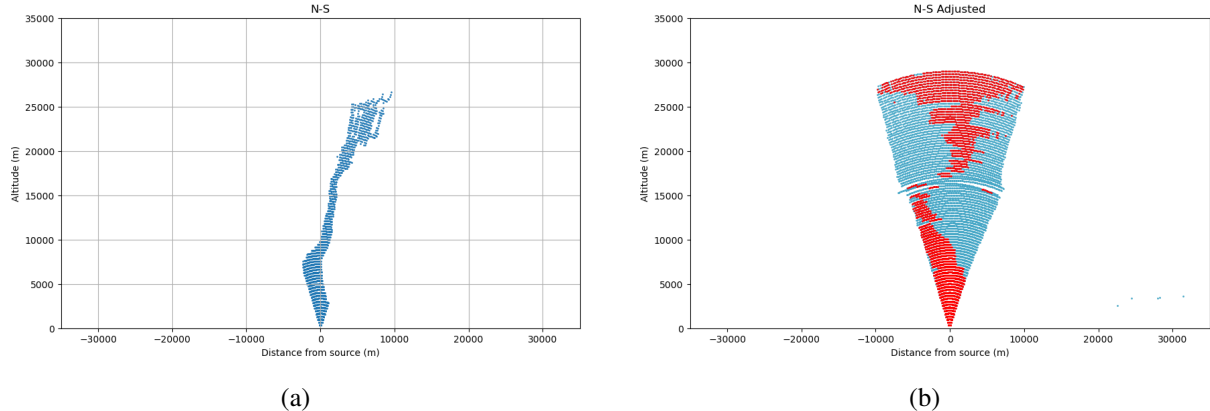


Figure 2.58: showed in the N-S plane

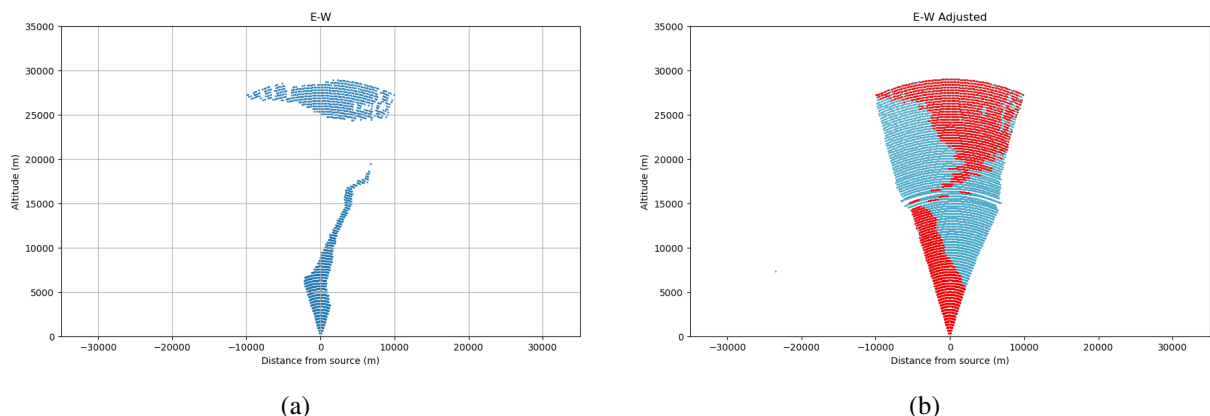


Figure 2.59: showed in the E-W plane

Assuming we take the top 10 windows for each wavefront, we need to find the next wavefront source location closest to the antenna array. Using this approach, the graphs will be as follows:

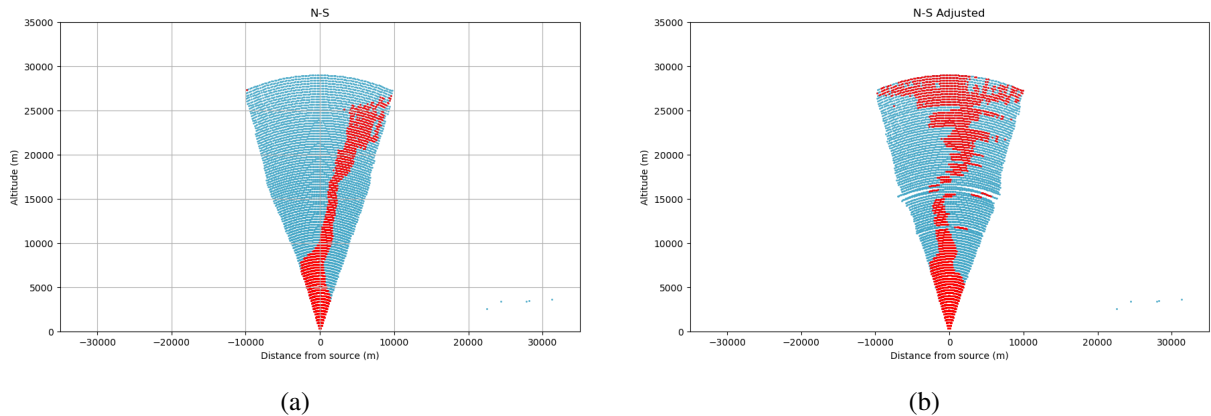


Figure 2.60: showed in the N-S plane

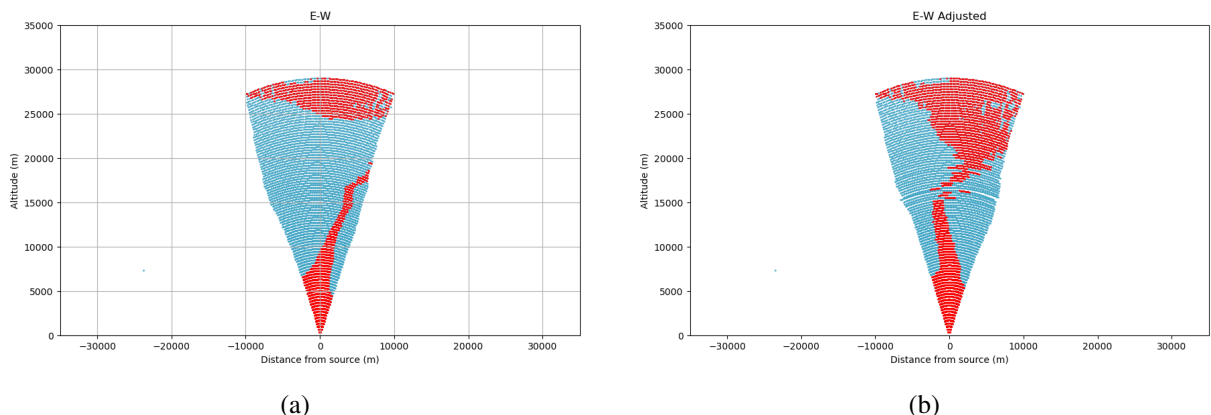


Figure 2.61

Now plotting the chosen source for each wavefront

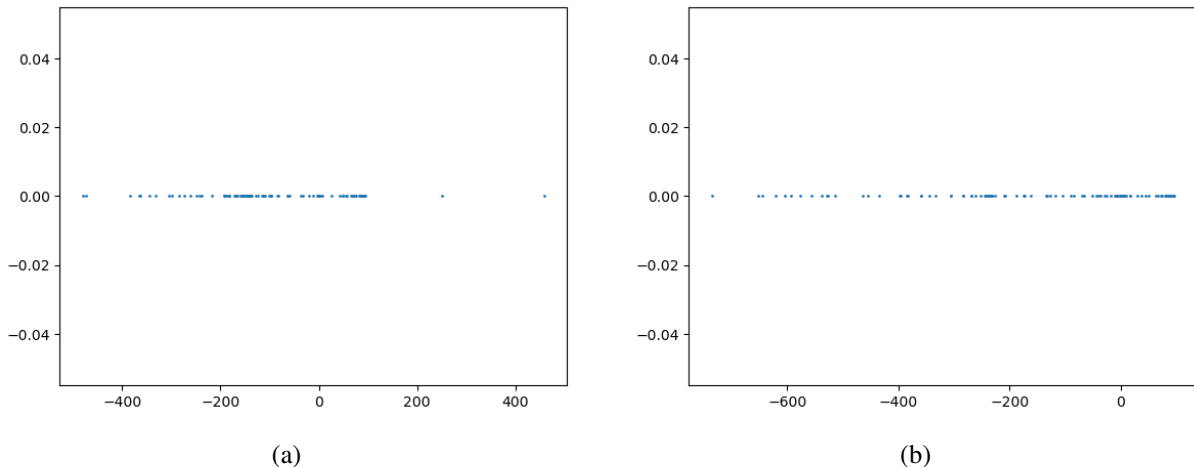


Figure 2.62

By using the DBSCAN clustering algorithm

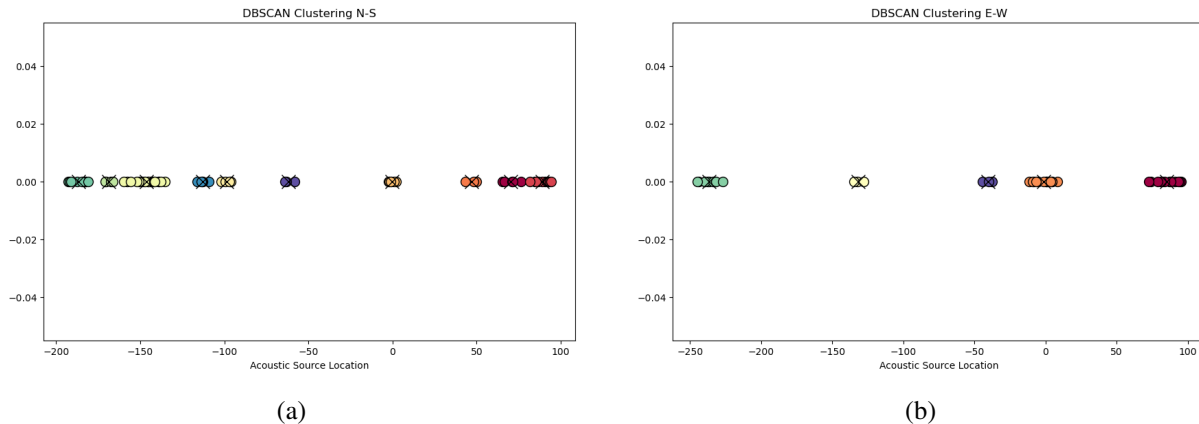


Figure 2.63

Now, by placing the sources at the locations determined by the clustering algorithm and overlapping all the backscattering from these sources, we obtain the following graph:

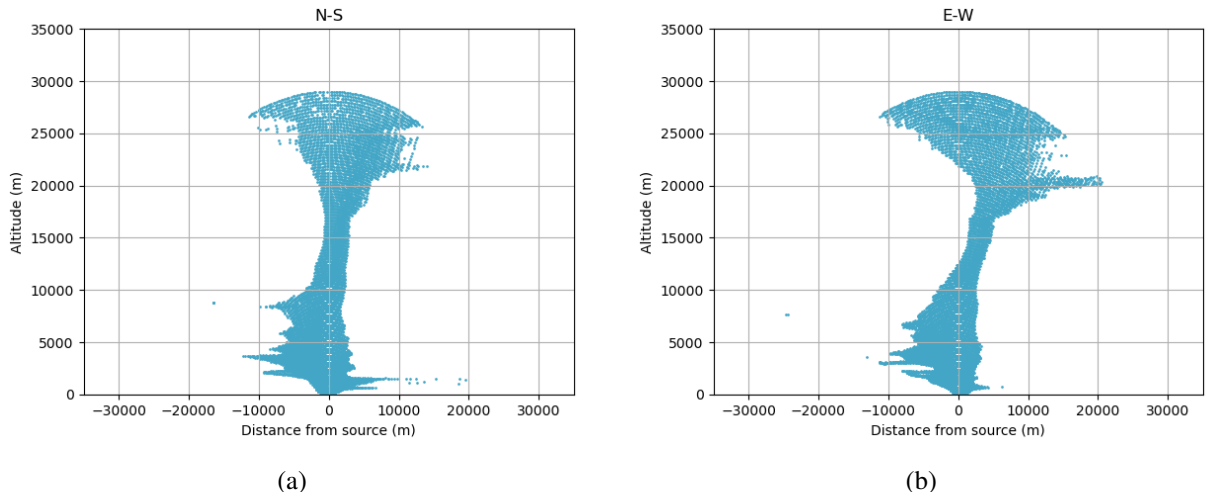


Figure 2.64

The image illustrates a combination of three elements: the blue area signifies the maximum coverage of the antenna array, the brown area represents the region where the backscatter falls within this coverage, and the cone section outlined by the green lines depicts the portion of the coverage that the antenna array can cover at any given time, which we aim to maximize it.

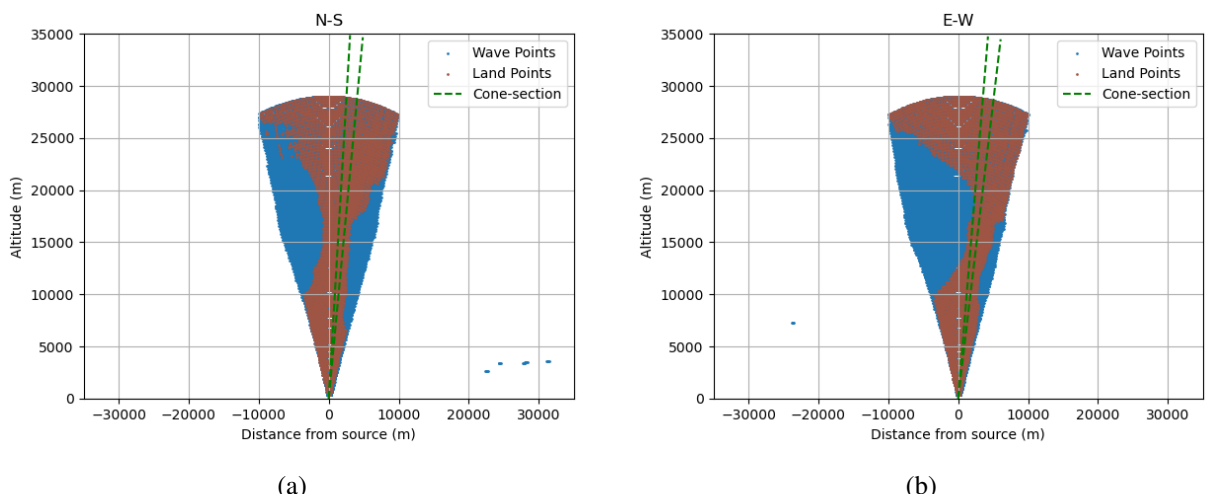


Figure 2.65

This page was intentionally left blank.

# **Chapter 3**

## **Results and Analysis**

### **3.1 Simulation**

We utilized Radiosonde data from 2021 to simulate and determine optimal acoustic source locations. The dataset included height, temperature, wind speed, and wind direction measurements for each day. By applying the design methodology outlined in Chapter 2, we identified and optimized the acoustic source locations for the entire year. This approach allowed us to evaluate the performance and effectiveness of our design in real-world atmospheric conditions.

### **3.2 Simulation Results**

In our study, simulations were conducted across both the North-South (N-S) and East-West (E-W) planes using radiosonde data from the year 2021.

<b>Month</b>	<b>Mean</b>	<b>Std</b>	<b>Min</b>	<b>25%</b>	<b>50%</b>	<b>75%</b>	<b>Max</b>
<b>Jan</b>	-121.57	171.35	-608.88	-246.52	-63.81	18.97	95.65
<b>Feb</b>	-103.81	144.80	-498.48	-185.56	-62.54	1.37	306.31
<b>Mar</b>	-53.29	116.35	-488.87	-99.58	-1.50	27.98	87.53
<b>Apr</b>	-73.03	129.00	-575.65	-155.50	-25.34	24.19	120.88
<b>May</b>	-47.88	99.73	-475.31	-98.86	-27.53	28.57	99.71
<b>Jun</b>	-52.94	102.87	-346.68	-103.33	-24.98	22.34	90.19
<b>Jul</b>	-47.12	104.43	-469.23	-86.73	-21.90	26.31	114.23
<b>Aug</b>	-47.32	99.28	-460.00	-98.31	-20.01	29.28	82.69
<b>Sep</b>	-30.01	79.13	-309.03	-74.01	-16.92	29.10	227.09
<b>Oct</b>	-61.85	111.01	-456.44	-119.44	-34.98	18.40	134.18
<b>Nov</b>	-70.65	137.75	-525.38	-156.42	-18.36	31.05	129.17
<b>Dec</b>	-49.05	125.39	-476.31	-108.49	-0.37	44.45	100.53

Table 3.1: Monthly Statistics in the N-S plane

<b>Month</b>	<b>Mean</b>	<b>Std</b>	<b>Min</b>	<b>25%</b>	<b>50%</b>	<b>75%</b>	<b>Max</b>
<b>Jan</b>	-28.89	123.91	-482.48	-81.86	-0.20	53.80	176.87
<b>Feb</b>	-227.12	301.71	-997.93	-459.65	-86.34	18.24	88.58
<b>Mar</b>	-48.78	158.49	-458.71	-128.22	0.45	66.00	250.52
<b>Apr</b>	-94.22	157.85	-626.88	-180.17	-38.94	23.39	106.56
<b>May</b>	-50.42	124.04	-549.74	-82.60	-2.09	30.14	139.61
<b>Jun</b>	-16.96	95.59	-313.10	-60.46	-1.67	32.47	463.78
<b>Jul</b>	-26.21	109.70	-367.47	-74.55	-21.85	25.56	693.32
<b>Aug</b>	25.05	149.01	-155.40	-46.22	0.14	42.09	765.40
<b>Sep</b>	-0.64	102.05	-193.11	-52.44	-1.04	41.01	462.52
<b>Oct</b>	37.91	87.75	-117.53	-4.62	26.28	64.08	458.52
<b>Nov</b>	55.37	77.05	-129.94	1.44	57.21	92.83	336.77
<b>Dec</b>	-102.04	231.39	-927.29	-171.22	-0.81	52.60	136.28

Table 3.2: Monthly Statistics in the E-W plane

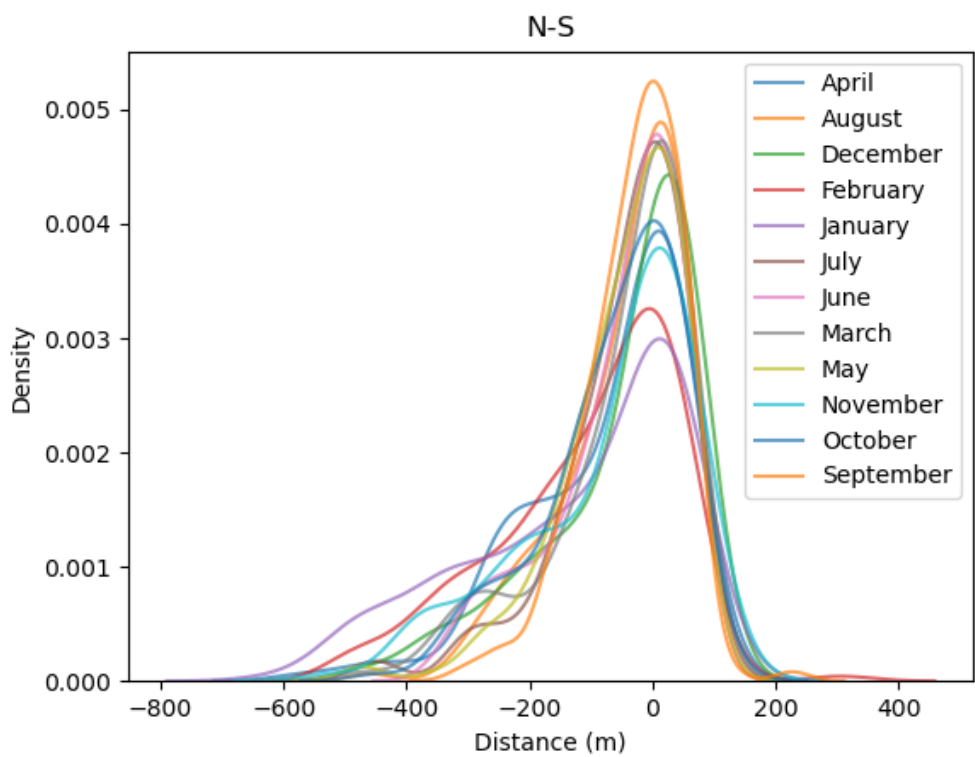


Figure 3.1: KDE plot for each month on N-S axis

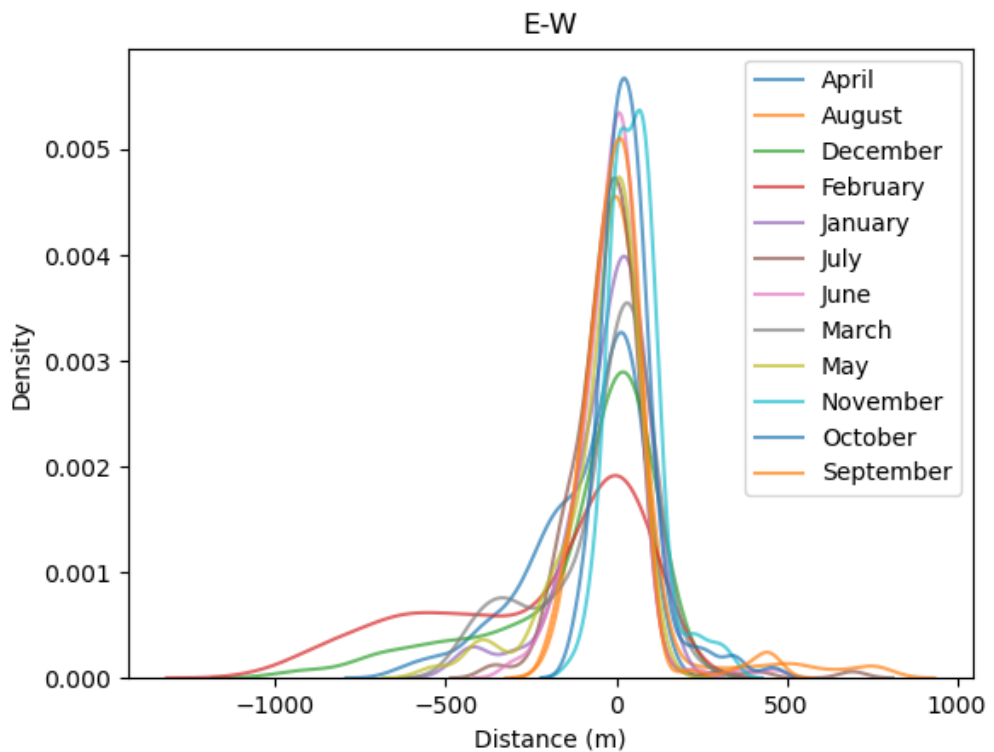


Figure 3.2: KDE plot for each month on E-W axis

### **3.3 Conclusion**

Through systematic simulation and analysis in both N-S and E-W planes using radiosonde data for the year 2021, we successfully optimized acoustic source locations for enhancing the performance of Radio Acoustic Sounding Systems (RASS). By leveraging atmospheric data to inform our design methodology, we achieved strategic placement of acoustic sources near the antenna array, as evidenced by consistent distributions observed in KDE plots across different months. This approach ensures efficient backscattering and maximizes coverage within the antenna array, thereby improving the accuracy and reliability of temperature and wind profile measurements. Moving forward, this methodology can be further refined to accommodate varying atmospheric conditions and enhance operational capabilities in atmospheric monitoring and research.

# **Appendix A**

## **Codes and Developed Tools**

### **A.1 RASS Acoustic Source Location Optimization**

A comprehensive framework for optimizing the placement of acoustic sources in a Radio Acoustic Sounding System (RASS) was developed. This framework leverages ray-tracing techniques and clustering algorithms to enhance the height coverage and accuracy of virtual temperature profiles. The entire processing chain for this optimization is implemented using Python, c++ and can be accessed through a GitHub repository for further use and development.

Inputs to this processing chain include (1) Daily radiosonde data for the year 2021, which provides atmospheric profiles such as height, temperature, wind speed, and wind direction, and (2) The dimensions of the radar antenna array. The framework simulates the propagation of acoustic wavefronts in an inhomogeneous atmosphere, considering temperature gradients and horizontal wind effects. After identifying optimal acoustic source locations, the results are analyzed and visualized using KDE plots to assess their effectiveness.

The optimized acoustic source locations are calculated and stored in CSV format, which can be used for further analysis or direct implementation in RASS setups.

## A.2 Simulation and Results Analysis

A robust simulation framework was developed to evaluate the performance of various acoustic source configurations in both North-South (N-S) and East-West (E-W) planes. This framework utilizes Python for the simulation and subsequent analysis, ensuring that the acoustic sources are strategically placed to maximize height coverage and backscatter efficiency.

Inputs to this processing chain are (1) Daily radiosonde data for the year 2021, (2) The predefined radar antenna array dimensions, and (3) Configuration parameters for the sliding window and clustering algorithms. The simulation framework systematically evaluates different acoustic source placements, applying the sliding window technique to optimize coverage and clustering algorithms to refine source positions.

The results are visualized through KDE plots, which illustrate the distribution of optimal acoustic source locations for each month. These plots help in understanding the consistency and effectiveness of the source placements throughout the year.

The final analysis demonstrates significant improvements in the continuous backscattering with respect to height and provides insights into the optimal deployment strategies for RASS acoustic sources.

## **List of Tables**

3.1	Monthly Statistics in the N-S plane . . . . .	48
3.2	Monthly Statistics in the E-W plane . . . . .	48

This page was intentionally left blank.

# List of Figures

1.1	Acoustic wavefronts in the absence of wind and temperature . . . . .	3
1.2	Acoustic wavefronts computer using temperature data . . . . .	3
1.3	Acoustic wavefronts computer using temperature data and wind data in N-S direction . . . . .	4
1.4	Acoustic wavefronts computer using temperature data and wind data in E-W direction . . . . .	4
1.5	Portions of acoustic wavefronts in the EW plane from which backscatter would fall on the antenna array computed using the radiosonde flight data . . . . .	5
1.6	Portions of acoustic wavefronts in the NS plane from which backscatter would fall on the antenna array computed using the radiosonde flight data . . . . .	5
2.1	Acoustic Source Locations around the antenna array of 130 x130 meters . . . . .	10
2.2	When the source is at the Origin, the portions of acoustic wavefronts in the NS plane from which backscatter would fall on the antenna array . . . . .	11
2.3	When the source is at the Origin, the portions of acoustic wavefronts in the EW plane from which backscatter would fall on the antenna array . . . . .	11
2.4	When the source is at the Bottom Left corner, the portions of acoustic wavefronts in the NS plane from which backscatter would fall on the antenna array . .	12
2.5	When the source is at the Bottom Left corner, the portions of acoustic wavefronts in the EW plane from which backscatter would fall on the antenna array .	12

2.6 When the source is at the bottom right corner, the portions of acoustic wavefronts in the NS plane from which backscatter would fall on the antenna array . . . . .	13
2.7 When the source is at the bottom right corner, the portions of acoustic wavefronts in the EW plane from which backscatter would fall on the antenna array . . . . .	13
2.8 When the source is at the top right corner, the portions of acoustic wavefronts in the NS plane from which backscatter would fall on the antenna array . . . . .	14
2.9 When the source is at the top right corner, the portions of acoustic wavefronts in the EW plane from which backscatter would fall on the antenna array . . . . .	14
2.10 When the source is at the top left corner, the portions of acoustic wavefronts in the NS plane from which backscatter would fall on the antenna array . . . . .	15
2.11 When the source is at the top left corner, the portions of acoustic wavefronts in the EW plane from which backscatter would fall on the antenna array . . . . .	15
2.12 When the source is at the bottom edge, the portions of acoustic wavefronts in the NS plane from which backscatter would fall on the antenna array . . . . .	16
2.13 When the source is at the bottom edge, the portions of acoustic wavefronts in the EW plane from which backscatter would fall on the antenna array . . . . .	16
2.14 When the source is at the right edge, the portions of acoustic wavefronts in the NS plane from which backscatter would fall on the antenna array . . . . .	17
2.15 When the source is at the right edge, the portions of acoustic wavefronts in the EW plane from which backscatter would fall on the antenna array . . . . .	17
2.16 When the source is at the top edge, the portions of acoustic wavefronts in the NS plane from which backscatter would fall on the antenna array . . . . .	18
2.17 When the source is at the top edge, the portions of acoustic wavefronts in the EW plane from which backscatter would fall on the antenna array . . . . .	18
2.18 When the source is at the left edge, the portions of acoustic wavefronts in the NS plane from which backscatter would fall on the antenna array . . . . .	19
2.19 When the source is at the left edge, the portions of acoustic wavefronts in the EW plane from which backscatter would fall on the antenna array . . . . .	19
2.20 When the sources are at the origin and bottom left corner, the portions of acoustic wavefronts in the NS plane from which backscatter would fall on the antenna array . . . . .	20
2.21 When the source is at the origin and bottom left corner, the portions of acoustic wavefronts in the EW plane from which backscatter would fall on the antenna array . . . . .	20

2.22 When the sources are at the origin and bottom right corner, the portions of acoustic wavefronts in the NS plane from which backscatter would fall on the antenna array . . . . .	21
2.23 When the source is at the origin and bottom right corner, the portions of acoustic wavefronts in the EW plane from which backscatter would fall on the antenna array . . . . .	21
2.24 When the sources are at the origin and top right corner, the portions of acoustic wavefronts in the NS plane from which backscatter would fall on the antenna array . . . . .	22
2.25 When the source is at the origin and top right corner, the portions of acoustic wavefronts in the EW plane from which backscatter would fall on the antenna array . . . . .	22
2.26 When the sources are at the origin and top left corner, the portions of acoustic wavefronts in the NS plane from which backscatter would fall on the antenna array . . . . .	23
2.27 When the source is at the origin and top left corner, the portions of acoustic wavefronts in the EW plane from which backscatter would fall on the antenna array . . . . .	23
2.28 When the sources are at the origin and bottom edge, the portions of acoustic wavefronts in the NS plane from which backscatter would fall on the antenna array . . . . .	24
2.29 When the source is at the origin and bottom edge, the portions of acoustic wavefronts in the EW plane from which backscatter would fall on the antenna array . . . . .	24
2.30 When the sources are at the origin and right edge, the portions of acoustic wavefronts in the NS plane from which backscatter would fall on the antenna array . . . . .	25
2.31 When the source is at the origin and right edge, the portions of acoustic wavefronts in the EW plane from which backscatter would fall on the antenna array . . . . .	25
2.32 When the sources are at the origin and top edge, the portions of acoustic wavefronts in the NS plane from which backscatter would fall on the antenna array . . . . .	26
2.33 When the source is at the origin and top edge, the portions of acoustic wavefronts in the EW plane from which backscatter would fall on the antenna array . . . . .	26
2.34 When the sources are at the origin and left edge, the portions of acoustic wavefronts in the NS plane from which backscatter would fall on the antenna array . . . . .	27
2.35 When the source is at the origin and left edge, the portions of acoustic wavefronts in the EW plane from which backscatter would fall on the antenna array . . . . .	27

2.36 When the sources are at the origin, bottom left corner, and top right corner, the portions of acoustic wavefronts in the NS plane from which backscatter would fall on the antenna array . . . . .	28
2.37 When the source is at the origin, bottom left corner, and top right corner, the portions of acoustic wavefronts in the EW plane from which backscatter would fall on the antenna array . . . . .	28
2.38 When the sources are at the origin, bottom right corner, and top left corner, the portions of acoustic wavefronts in the NS plane from which backscatter would fall on the antenna array . . . . .	29
2.39 When the source is at the origin, bottom right corner, and top left corner, the portions of acoustic wavefronts in the EW plane from which backscatter would fall on the antenna array . . . . .	29
2.40 When the sources are at the origin, bottom edge, and top edge, the portions of acoustic wavefronts in the NS plane from which backscatter would fall on the antenna array . . . . .	30
2.41 When the source is at the origin, bottom edge, and top edge, the portions of acoustic wavefronts in the EW plane from which backscatter would fall on the antenna array . . . . .	30
2.42 When the sources are at the origin, right edge, and left edge, the portions of acoustic wavefronts in the NS plane from which backscatter would fall on the antenna array . . . . .	31
2.43 When the source is at the origin, right edge, and left edge, the portions of acoustic wavefronts in the EW plane from which backscatter would fall on the antenna array . . . . .	31
2.44 When the sources are at the origin and all the corners, the portions of acoustic wavefronts in the NS plane from which backscatter would fall on the antenna array . . . . .	32
2.45 When the source is at the origin, and all the corners, the portions of acoustic wavefronts in the EW plane from which backscatter would fall on the antenna array . . . . .	32
2.46 When the sources are at the origin, and all the edges, the portions of acoustic wavefronts in the NS plane from which backscatter would fall on the antenna array . . . . .	33

2.47 When the source is at the origin, and all the edges, the portions of acoustic wavefronts in the EW plane from which backscatter would fall on the antenna array . . . . .	33
2.48 When the sources are at the origin, all corners and edges, the portions of acoustic wavefronts in the NS plane from which backscatter would fall on the antenna array . . . . .	34
2.49 When the source is at the origin, all corners and edges, the portions of acoustic wavefronts in the EW plane from which backscatter would fall on the antenna array . . . . .	34
2.50 Flowchart of the Design . . . . .	37
2.51 . . . . .	38
2.52 . . . . .	38
2.53 . . . . .	39
2.54 . . . . .	39
2.55 . . . . .	40
2.56 showed in the N-S plane . . . . .	41
2.57 showed in the E-W plane . . . . .	41
2.58 showed in the N-S plane . . . . .	42
2.59 showed in the E-W plane . . . . .	42
2.60 showed in the N-S plane . . . . .	43
2.61 . . . . .	43
2.62 . . . . .	44
2.63 . . . . .	44
2.64 . . . . .	45
2.65 . . . . .	45
3.1 KDE plot for each month on N-S axis . . . . .	49
3.2 KDE plot for each month on E-W axis . . . . .	49

This page was intentionally left blank.

# Acknowledgments

This project represents the culmination of research conducted since May 20, 2024 as part of my Bachelor of Technology. Over this period, I have received tremendous support and guidance from numerous individuals, to whom I am deeply grateful.

First and foremost, I would like to express my sincere gratitude to my thesis supervisor, Dr. T. V. Chandrasekhar Sarma, for their unwavering support, invaluable guidance, and continuous encouragement throughout my research journey, whose insights and expertise have been instrumental in shaping this work.

I am extremely thankful to Prof. Nityananda Nandi, Head of the department, Aerospace Engineering and Applied Mechanics, Indian Institute of Engineering Science and Technology, Shibpur for helping me get this auspicious opportunity.

Thank you all for being part of this incredible journey.

**Signature of Student:** Ypati Murali Sai

Ypati Murali Sai  
Department of Aerospace Engineering and Applied Mechanics  
Indian Institute of Engineering Science and Technology